Arbitrary Lagrangian–Eulerian (ALE) Formulation

Theory, Numerical Methods, and Applications

Hua-Dong Yao

Department of Mechanical Engineering
Chalmers University of Technology
SE-412 96, Gothenburg, Sweden

huadong.yao@chalmers.se

March 27, 2026

Technical Report: TR-2026-01
DOI: 10.63959/m2.techreport/2026.1
URL: https://research.chalmers.se/publication/551352

Abstract

This report presents a systematic formulation of the Arbitrary Lagrangian–Eulerian (ALE) framework for continuum mechanics problems involving time-dependent domains. Such problems arise naturally in fluid–structure interaction (FSI), free-surface flows, and other applications where the computational domain evolves as part of the solution. The central challenge is the consistent formulation of conservation laws when the domain $\Omega(t)$ is itself a function of time. To address this, the ALE description introduces a kinematic decoupling between material motion and mesh motion, enabling a unified treatment that bridges classical Lagrangian and Eulerian viewpoints. Starting from first principles, the full set of conservation laws (mass, momentum, and energy) is reformulated on moving domains, leading to the ALE Reynolds Transport Theorem and the corresponding governing equations expressed in terms of the relative (convective) velocity $\mathbf{c} = \mathbf{v} - \mathbf{w}$, where $\mathbf{v}$ is the material velocity and $\mathbf{w}$ is the mesh velocity. Particular emphasis is placed on the Geometric Conservation Law (GCL), which provides a necessary consistency condition between mesh motion and volume evolution to ensure numerical stability and accuracy. Both continuous and discrete forms of the GCL are discussed, highlighting their role in preventing spurious sources in moving-mesh simulations. The report covers both major spatial discretization strategies for moving-domain problems. For finite element methods, the variational ALE form is derived, and Streamline-Upwind Petrov–Galerkin (SUPG) and Pressure-Stabilizing Petrov–Galerkin (PSPG) stabilizations are formulated in terms of the relative velocity. For finite volume methods, the ALE flux construction and donor-cell reconstruction strategies are presented alongside the DGCL-consistent time integration algorithm. Mesh motion strategies are surveyed, including spring analogy, Laplacian smoothing, and elastic analogy methods, together with mesh quality metrics that guide the choice of remeshing strategy. The report further interprets the ALE framework in the context of fluid–structure interaction, where boundary-fitted meshes enable high-fidelity resolution of interface physics. Finally, the advantages and limitations of ALE are critically assessed, with comparisons to alternative approaches such as fixed-grid and immersed methods, providing guidance on the appropriate use of ALE in practical simulations.

Contents

1 Introduction and Motivation

1.1 Moving Boundary Problems

Many problems in continuum mechanics involve domains that evolve over time. Instead of a fixed spatial region, the computational domain must be described as a time-dependent set $\Omega(t)$, whose boundary $\partial\Omega(t)$ changes as part of the solution.

Such situations arise in a wide range of engineering applications. In fluid–structure interaction (FSI), the deformation of a structure directly modifies the surrounding fluid domain [Donea et al., 1982]. In free-surface flows, such as ocean waves or sloshing tanks, the interface between phases evolves continuously. Similarly, in phase-change problems, including melting and solidification, the boundary between phases moves as a result of energy transfer.

From a mathematical perspective, these problems are characterized by the condition

$$\frac{\partial\Omega}{\partial t} \neq 0, \tag{1}$$

which indicates that the domain itself is a function of time.

This situation introduces a fundamental conceptual and mathematical difficulty. Classical conservation laws are formulated with respect to a control volume that is fixed in space, which allows the time rate of change of a conserved quantity to be expressed solely in terms of fluxes across a stationary boundary and sources within the domain. When the control volume itself becomes time-dependent, this standard formulation is no longer directly applicable and must be generalized to account for the motion and deformation of the domain.

In a moving control volume, the variation of a physical quantity cannot be attributed to a single mechanism. Instead, two distinct but coupled effects must be considered. On one hand, the quantity may change due to physical transport processes such as advection and diffusion within the domain, as well as fluxes across its boundary. On the other hand, the geometry of the control volume may evolve in time, altering both its size and shape. This geometric evolution contributes to the overall rate of change even in the absence of any physical transport, since the domain over which the quantity is defined is itself varying.

A consistent formulation of conservation laws in such settings therefore requires a clear separation between these two contributions, followed by their rigorous combination. This distinction is central to the development of the Arbitrary Lagrangian–Eulerian (ALE) framework, where the relative motion between the material, the control volume, and the reference frame must be carefully accounted for in order to preserve the correct balance relations.

1.2 Classical Descriptions: Lagrangian and Eulerian

Before introducing the Arbitrary Lagrangian–Eulerian formulation, it is instructive to revisit the two classical descriptions of motion in continuum mechanics. These two viewpoints differ fundamentally in how the computational domain is defined and how the motion of the material is represented, and each leads to a distinct interpretation of the governing equations.

1.2.1 Lagrangian description

In the Lagrangian framework, the computational mesh is attached to the material and therefore moves with it. Each mesh node is identified with a specific material particle, and its trajectory follows the material motion according to

$$\frac{d\mathbf{x}}{dt} = \mathbf{v}, \tag{2}$$

where $\mathbf{v}$ denotes the material velocity. In this description, the deformation of the continuum is directly reflected in the deformation of the mesh.

A key advantage of the Lagrangian approach is its natural ability to represent moving boundaries and interfaces exactly. Since the mesh conforms to the material at all times, interfaces remain sharp and well-resolved without the need for additional reconstruction or tracking techniques. This property is particularly valuable in problems involving free surfaces or fluid–structure interaction.

However, this tight coupling between mesh and material motion also introduces significant limitations. In situations involving large deformations, the mesh may undergo severe distortion. Elements can become highly skewed or stretched, and in extreme cases may invert, leading to a breakdown of the numerical discretization. As a consequence, the accuracy and stability of the computation can deteriorate rapidly unless frequent and potentially costly remeshing procedures are employed.

1.2.2 Eulerian description

In contrast, the Eulerian framework adopts a spatially fixed computational mesh. The governing equations are formulated at fixed points in space, and the material flows through the grid. The primary unknowns, such as velocity and pressure, are therefore interpreted as fields defined over a stationary domain.

This description offers a high degree of robustness in problems involving large deformations or complex flow patterns. Since the mesh does not move or deform, its quality remains intact throughout the simulation, avoiding the numerical issues associated with mesh distortion. This makes the Eulerian approach particularly well suited for flows with significant topological changes or strong convective effects.

The main limitation of the Eulerian framework lies in its treatment of interfaces and moving boundaries. Because the mesh is not aligned with the material, interfaces are not explicitly tracked and must instead be represented indirectly, often leading to numerical diffusion. As a result, sharp features such as material discontinuities or free surfaces may become smeared over several computational cells, reducing the accuracy of the solution in regions where precise interface resolution is essential.

1.2.3 Fundamental trade-off

The Lagrangian and Eulerian descriptions thus embody two complementary perspectives. The former provides an exact kinematic description of material motion and naturally preserves interface sharpness, but suffers from mesh degradation under large deformation. The latter maintains a high-quality mesh regardless of the flow, but sacrifices the ability to represent interfaces sharply without additional modeling techniques.

This inherent trade-off motivates the development of hybrid formulations that aim to combine the advantages of both approaches. The Arbitrary Lagrangian–Eulerian framework emerges from this need [Hirt et al., 1974, Hughes et al., 1981, Donea et al., 1982], introducing additional flexibility in the choice of mesh motion while retaining a consistent description of the underlying physical processes.

1.3 The ALE Framework

The Arbitrary Lagrangian–Eulerian (ALE) formulation is a continuous generalization of the two classical viewpoints in continuum mechanics. Its core philosophy is the decoupling of the computational mesh from the material trajectory, introducing an additional degree of freedom that allows the grid to move independently of the physical flow. This flexibility is exploited to maintain high numerical performance while preserving a consistent physical description, even under significant domain evolution.

The ALE framework may be interpreted as a unified setting that balances the accurate interface tracking of Lagrangian methods against the topological robustness of Eulerian discretizations. By allowing the mesh to move arbitrarily, subject only to the requirement that it remains a valid diffeomorphism, the solver can adapt to complex geometries without inheriting the full, often destructive, deformation of the material. As a result, the classical descriptions are recovered as simple limiting cases:

- **Eulerian:** The mesh remains fixed in space, and the formulation tracks material flux through stationary volumes.
- **Lagrangian:** The mesh follows the material perfectly, and the formulation tracks the deformation of fixed material parcels.

By occupying the middle ground between these limits, ALE provides the necessary infrastructure for simulations where the boundary motion is known or critical, but the interior flow remains complex and highly deforming.

1.4 Kinematic Interpretation

The conceptual independence of the ALE framework is realized through a specific kinematic structure. We distinguish between the material velocity $\mathbf{v}$, defining where the fluid "wants" to go, and the mesh velocity $\mathbf{w}$, which represents the algorithmically determined trajectory of the grid points. Their vector difference defines the relative (or convective) velocity:

$$\mathbf{c} = \mathbf{v} - \mathbf{w}. \tag{3}$$

As illustrated in Figure 1, this relative velocity serves as the effective flux perceived by the moving mesh. It dictates that advective transport is driven not by the absolute motion of the material, but by its motion relative to the evolving computational frame.

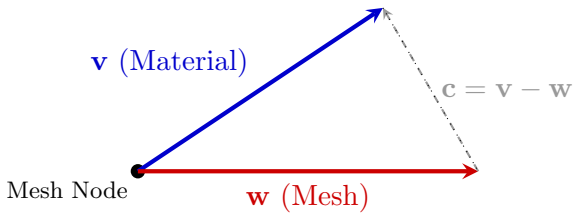

Figure 1: Vector relationship between material velocity $\mathbf{v}$, mesh velocity $\mathbf{w}$, and the resulting convective velocity $\mathbf{c}$.

The implications for the governing equations are immediate. In a classical Eulerian setting, the convective term in the momentum equation is expressed as $\mathbf{v} \cdot \nabla \mathbf{v}$. Within the ALE framework, this term is modified to reflect the relative transport:

$$(\mathbf{v} - \mathbf{w}) \cdot \nabla \mathbf{v}. \tag{4}$$

This mathematical shift has profound numerical consequences. In regions where the mesh is prescribed to follow the material motion ($\mathbf{w} \approx \mathbf{v}$), the relative velocity $\mathbf{c}$ approaches zero. This reduction in effective convective strength directly diminishes numerical diffusion in the computational frame, allowing the ALE formulation to maintain sharp interfaces and boundary layers that would otherwise be smoothed out in a purely Eulerian discretization.

1.5 Advantages and Scope of ALE

The Arbitrary Lagrangian–Eulerian framework represents a high-performance synthesis of the classical Lagrangian and Eulerian descriptions, designed specifically to mitigate their respective shortcomings. By allowing the mesh to move independently of the material velocity, ALE provides a unique "User-Defined" mesh quality that is absent in fixed-grid or purely material-tracking methods. The comparative strengths of the ALE approach are summarized in Table 1.

Table 1: Comparative analysis of kinematic descriptions.

Feature	**Lagrangian**	**Eulerian**	**ALE**
Large Deformations	Low	High	**High**
Interface Resolution	High	Low	**High**
Mesh Quality	Poor	Fixed	**User-Defined**
Physical Intuition	High	Moderate	**Hybrid**

The primary advantage of the ALE formulation lies in its ability to enable the accurate tracking of moving boundaries and interfaces. Because the mesh can be prescribed to follow the motion of the domain where needed, it preserves sharp geometric features without the excessive numerical diffusion typically associated with interface-capturing methods on fixed grids. Furthermore, the framework maintains high mesh quality even under moderate to large deformations. Since the mesh motion is a controllable variable, distortions that would otherwise lead to element inversion in a Lagrangian setting can be redistributed or smoothed throughout the domain.

This inherent flexibility allows practitioners to tailor the mesh motion to the specific requirements of the problem, for instance by concentrating spatial resolution in regions of high gradients or aligning the mesh with dominant flow features. Consequently, ALE has become the gold standard for Fluid–Structure Interaction (FSI) and free-surface problems, where the boundary motion is either known a priori or must be computed iteratively as part of the coupled solution [Donea et al., 2004].

However, the applicability of ALE is naturally bounded by the topological limits of the mesh. When a problem involves extreme deformations, rapid changes in connectivity, or the creation and destruction of interfaces (such as wave breaking or structural fragmentation), maintaining a valid mapping becomes increasingly difficult. In these specific regimes, the computational overhead of frequent remeshing may outweigh the accuracy benefits, and alternative fixed-grid or interface-capturing techniques may offer a more robust solution. Nevertheless, for the vast majority of continuous moving-boundary problems, the ALE method remains the most balanced approach for achieving both geometric precision and numerical stability.

2 Kinematics and Mapping in ALE

2.1 Reference and Physical Domains

A precise formulation of the Arbitrary Lagrangian–Eulerian framework requires a clear distinction between the domain used for description and the domain in which the physical problem is posed. To this end, we introduce a fixed *reference domain* $\hat{\Omega}$ and a time-dependent *physical domain* $\Omega(t)$. The latter represents the actual configuration of the continuum at time t, while the former serves as a stationary computational frame that provides a convenient parameterization of the evolving geometry.

Rather than formulating the governing equations directly on the moving domain, the ALE

approach represents the geometric evolution through a time-dependent mapping:

$$\mathbf{x} = \boldsymbol{\chi}(\hat{\mathbf{x}}, t) \tag{5}$$

where $\hat{\mathbf{x}} \in \hat{\Omega}$ denotes the referential coordinates and $\mathbf{x} \in \Omega(t)$ denotes the corresponding spatial coordinates. This mapping establishes a one-to-one correspondence between the fixed reference configuration and the current physical configuration at each instant in time, as illustrated in Figure 2.

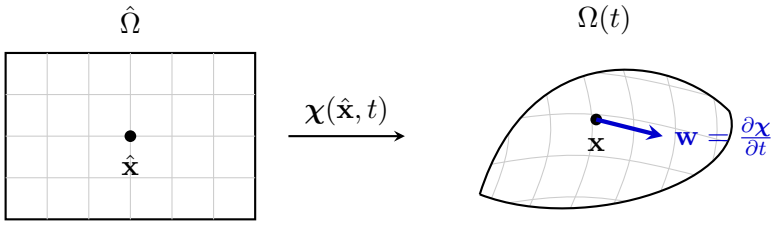

Figure 2: The ALE mapping $\boldsymbol{\chi}$ transports the computational mesh from the structured reference domain $\hat{\Omega}$ to the physical domain $\Omega(t)$, inducing a mesh velocity $\mathbf{w}$ at the spatial coordinates.

As depicted, the function $\boldsymbol{\chi}$ encapsulates the motion of the computational mesh. It specifies how each point in the reference domain is transported into the physical domain as time evolves. Importantly, this mapping is purely geometric in nature and is not constrained to coincide with the material motion. This distinction is fundamental to the ALE formulation, as it enables an independent prescription of mesh movement.

From a computational perspective, the referential coordinate $\hat{\mathbf{x}}$ can be interpreted as a fixed label associated with each mesh node. The mapping $\boldsymbol{\chi}$ then determines the position of that node in physical space at any given time. The freedom to define $\boldsymbol{\chi}$ according to numerical considerations, such as preserving mesh quality or ensuring alignment with moving boundaries, underpins the flexibility of the ALE framework in practical engineering applications.

2.2 Mesh Velocity

The time dependence of the mapping $\boldsymbol{\chi}(\hat{\mathbf{x}}, t)$ introduces, in a natural way, the notion of *mesh velocity*. This quantity is defined as the time derivative of the mapping at fixed referential coordinates:

$$\mathbf{w}(\mathbf{x}, t) = \left.\frac{\partial \boldsymbol{\chi}}{\partial t}\right|_{\hat{\mathbf{x}}}. \tag{6}$$

It represents the velocity of the computational mesh points as they move through physical space. It is important to distinguish this velocity from the material velocity $\mathbf{v}$; while $\mathbf{v}$ describes the motion of physical particles, the mesh velocity $\mathbf{w}$ is purely geometric and reflects the evolution of the computational grid.

The classical descriptions of continuum mechanics are recovered as special cases corresponding to particular choices of $\mathbf{w}$, as illustrated in Figure 3.

As shown in the comparison, the **Eulerian** formulation assumes $\mathbf{w} = \mathbf{0}$, meaning the mesh remains fixed in space. This is computationally efficient for large-scale flows but forces interfaces to cut through cells. The **Lagrangian** formulation assumes $\mathbf{w} = \mathbf{v}$, where the mesh moves exactly with the material, allowing for precise interface tracking but risking mesh entanglement under large deformations.

The ALE formulation generalizes both viewpoints by allowing intermediate mesh motions where $\mathbf{v} \neq \mathbf{w} \neq \mathbf{0}$. This hybrid approach combines the strengths of both classical methods: it enables explicit interface tracking while allowing the interior mesh to be "smoothed" to remain healthy.

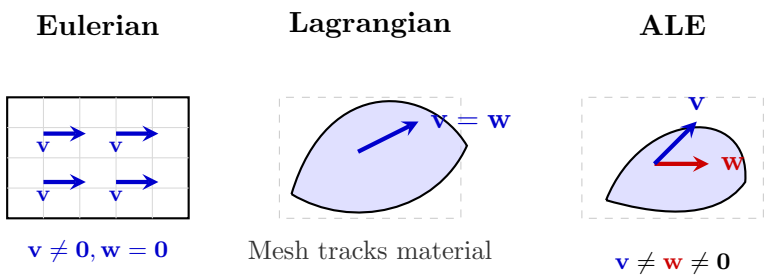

Figure 3: Comparison of Eulerian, Lagrangian, and ALE kinematic descriptions.

In practical computations, the mesh velocity is determined through an auxiliary mesh-motion model. These models are designed to produce smooth and well-behaved deformations of the grid while preserving element quality. Common approaches include the spring analogy [Batina, 1990] and linear elasticity analogies [Johnson and Tezduyar, 1994], where the mesh is treated as a fictitious continuum that deforms under prescribed boundary displacements. Through these mechanisms, the mesh motion can be controlled in a systematic manner, ensuring that the computational domain evolves without introducing excessive distortion or numerical degradation.

2.3 Deformation Gradient and Jacobian

The local geometric transformation induced by the mapping $\boldsymbol{\chi}(\hat{\mathbf{x}}, t)$ is characterized by the *deformation gradient*

$$\mathbf{F} = \frac{\partial \boldsymbol{\chi}}{\partial \hat{\mathbf{x}}} = \nabla_{\hat{\mathbf{x}}} \mathbf{x}. \tag{7}$$

This tensor describes how infinitesimal neighborhoods in the reference domain are mapped into the physical domain. In particular, it provides a linear approximation of the mapping in the vicinity of a given point.

More precisely, the deformation gradient relates differential line elements in the two configurations through

$$d\mathbf{x} = \mathbf{F}, d\hat{\mathbf{x}}, \tag{8}$$

which shows that $\mathbf{F}$ encodes both stretching and rotation of the mesh at the local level. It therefore captures the full kinematic information associated with the mesh deformation.

It is important to emphasize that, in the present context, $\mathbf{F}$ does not describe material deformation, as it would in classical solid mechanics. Instead, it quantifies the distortion of the computational mesh induced by the chosen mapping. The same mathematical object is thus reinterpreted in a purely geometric sense within the ALE framework.

A scalar measure of this local transformation is provided by the *Jacobian*

$$J(\hat{\mathbf{x}}, t) = \det(\mathbf{F}), \tag{9}$$

which represents the ratio of differential volume elements between the physical and reference configurations. This relation is made explicit through the transformation formula

$$dV = J, d\hat{V}, \tag{10}$$

which enables integrals over the time-dependent domain $\Omega(t)$ to be systematically mapped onto the fixed reference domain $\hat{\Omega}$. This property is fundamental for both analysis and numerical implementation, as it allows all computations to be performed on a stationary mesh while accounting for geometric evolution.

Beyond its role in coordinate transformation, the Jacobian also provides a direct measure of mesh quality. Values of J close to zero indicate severe compression of elements, potentially

leading to element degeneration or inversion. Such situations compromise both the accuracy and stability of the numerical scheme. For this reason, it is essential to ensure that the Jacobian remains strictly positive and sufficiently bounded throughout the computation, which in turn places constraints on the admissible mesh motion.

2.4 Referential Time Derivative

Within the ALE framework, the notion of a time derivative requires careful specification, as the choice of reference frame directly affects its interpretation. In particular, it is necessary to distinguish between derivatives taken at fixed spatial locations and those taken while following the motion of the computational mesh. This distinction reflects the fundamental separation between physical and geometric descriptions introduced earlier.

The *referential time derivative* is defined as

$$\left.\frac{\partial f}{\partial t}\right|_{\hat{\mathbf{x}}}, \tag{11}$$

and represents the rate of change of a field $f(\mathbf{x}, t)$ as observed at a fixed point in the reference domain. Equivalently, it corresponds to following a mesh node as it moves through physical space and recording how the field evolves along that trajectory.

To relate this derivative to quantities expressed in spatial coordinates, consider the composite function $f(\boldsymbol{\chi}(\hat{\mathbf{x}}, t), t)$. Application of the chain rule then yields

$$\left.\frac{\partial f}{\partial t}\right|_{\hat{\mathbf{x}}} = \frac{\partial f}{\partial t} + \mathbf{w} \cdot \nabla f, \tag{12}$$

where $\mathbf{w}$ is the mesh velocity. This expression provides a direct link between the referential and spatial descriptions.

The resulting identity has a clear interpretation. The first term, $\partial f/\partial t$, represents the local temporal variation of the field at a fixed point in space. The second term, $\mathbf{w} \cdot \nabla f$, accounts for the additional change induced by the motion of the mesh through spatial gradients of the field. The referential time derivative therefore combines intrinsic temporal variation with a transport effect associated with the displacement of the computational grid. This decomposition plays a central role in reformulating the governing equations on a moving domain.

2.5 Material Derivative in ALE Form

The material derivative expresses the rate of change of a field as experienced by a material particle moving with the flow. In the classical Eulerian description, it is written as

$$\frac{Df}{Dt} = \frac{\partial f}{\partial t} + \mathbf{v} \cdot \nabla f, \tag{13}$$

where the first term represents the local temporal variation at a fixed spatial point, and the second term accounts for advection due to the material velocity $\mathbf{v}$.

Within the ALE framework, it is convenient to reformulate this expression in terms of the referential time derivative introduced earlier. Substituting the relation between the referential and spatial derivatives yields

$$\frac{Df}{Dt} = \left.\frac{\partial f}{\partial t}\right|_{\hat{\mathbf{x}}} + (\mathbf{v} - \mathbf{w}) \cdot \nabla f. \tag{14}$$

This form separates the rate of change into two contributions that are naturally interpreted within a moving mesh context.

The quantity

$$\mathbf{c} = \mathbf{v} - \mathbf{w} \tag{15}$$

is referred to as the *convective velocity*. It represents the motion of material relative to the computational mesh and therefore governs the effective transport of quantities across the moving control volume.

This decomposition makes explicit the central idea underlying the ALE formulation. The physical evolution of a field is expressed as the sum of a time variation observed while following the mesh and a convective transport relative to that mesh. By separating these effects, the formulation provides a consistent framework for incorporating mesh motion into the governing equations while preserving their physical interpretation.

2.6 Evolution of the Jacobian

The temporal evolution of the Jacobian associated with the mapping $\boldsymbol{\chi}(\hat{\mathbf{x}}, t)$ is governed by the identity

$$\left.\frac{\partial J}{\partial t}\right|_{\hat{\mathbf{x}}} = J, (\nabla \cdot \mathbf{w}). \tag{16}$$

This relation provides a direct link between the rate of change of local volume and the kinematics of the mesh motion.

More specifically, the divergence of the mesh velocity $\mathbf{w}$ characterizes the local volumetric deformation of the computational grid. A positive value of $\nabla \cdot \mathbf{w}$ indicates that neighboring mesh points are moving away from each other, leading to a local expansion of the domain and an increase in J. Conversely, a negative divergence corresponds to compression, where mesh elements contract and the Jacobian decreases. In this sense, the above identity can be interpreted as a local conservation statement for volume under the mapping.

This result plays a fundamental role in the ALE formulation of conservation laws. It ensures that changes in the measure of the computational domain, as captured by the Jacobian, are consistently accounted for in the balance equations. Without this relation, the coupling between mesh motion and physical conservation would be incomplete, potentially leading to inconsistencies in the discrete formulation.

2.7 Geometric Conservation Law

A fundamental consistency requirement for numerical methods on moving meshes is the *Geometric Conservation Law* (GCL) [Lesoinne and Farhat, 1996]. In integral form, it states that the rate of change of a moving control volume $V(t)$ must be exactly balanced by the volumetric flux driven by the mesh velocity across its boundary $S(t)$:

$$\frac{d}{dt}\int_{V(t)} dV = \int_{S(t)} \mathbf{w} \cdot \mathbf{n}\, dS. \tag{17}$$

Its physical role is to ensure that purely geometric changes in the domain are never misinterpreted as physical sources or sinks of a conserved quantity. The continuous and discrete forms of the GCL, together with their implications for numerical stability, freestream preservation, and the design of time-stepping schemes, are developed in full in Section 6.

2.8 Transformation of Integrals

The mapping $\boldsymbol{\chi}(\hat{\mathbf{x}}, t)$ provides a systematic way to express integrals over the time-dependent physical domain in terms of the fixed reference domain. Specifically, a volume integral over $\Omega(t)$ can be rewritten as

$$\int_{\Omega(t)} f(\mathbf{x}, t), d\Omega = \int_{\hat{\Omega}} f(\boldsymbol{\chi}(\hat{\mathbf{x}}, t), t), J(\hat{\mathbf{x}}, t), d\hat{\Omega}, \tag{18}$$

where the Jacobian $J = \det(\mathbf{F})$ accounts for the local change of volume induced by the mapping. This transformation allows all integrals to be evaluated on a stationary domain, which is particularly advantageous for both analysis and numerical implementation.

The presence of the Jacobian introduces an additional layer of complexity when considering time-dependent problems. Since J depends explicitly on time through the mapping, it contributes to the temporal variation of the integral. As a result, differentiating such expressions requires careful application of the product rule, taking into account both the evolution of the integrand and the evolution of the domain measure.

This aspect is central to the derivation of conservation laws in the ALE framework. The interplay between the time dependence of the field variables and the geometric evolution encoded in J leads directly to the modified balance equations that incorporate mesh motion in a consistent and conservative manner.

3 ALE Conservation Laws and the Transport Identity

The fundamental challenge in simulating moving-domain problems, such as Fluid-Structure Interaction (FSI) or free-surface flows, lies in the fact that the spatial domain $\Omega(t)$ is time-dependent. In classical Eulerian CFD, the control volume is fixed in space, allowing the partial time derivative to commute with the integral operator. However, in the Arbitrary Lagrangian-Eulerian (ALE) framework, the boundaries and internal grid points deform, requiring a more sophisticated treatment of the conservation laws.

3.1 The Integration Problem on Deforming Domains

Consider a general scalar or vector field $\phi(\mathbf{x}, t)$, representing a physical quantity such as density, momentum, or energy, defined over a time-dependent spatial domain $\Omega(t)$. The total amount of this quantity within the domain is given by the integral:

$$\mathcal{I}(t) = \int_{\Omega(t)} \phi(\mathbf{x}, t)\, d\Omega. \tag{19}$$

This integral represents a global measure that evolves in time due to the simultaneous variation of the field itself and the geometric configuration of the domain.

A fundamental difficulty arises when attempting to compute the time derivative of $\mathcal{I}(t)$. Unlike integrals over fixed domains, the limits of integration here are time-dependent; consequently, the derivative cannot be obtained by simply differentiating the integrand. In a moving-frame context, the operation $\frac{d}{dt}\int_{\Omega(t)} \phi\, d\Omega$ does not reduce to $\int_{\Omega(t)} \frac{\partial \phi}{\partial t}\, d\Omega$, as the latter neglects the contribution arising from the motion of the domain boundary. To correctly evaluate this rate of change, one must account for two distinct physical effects, as visualized in Figure 4.

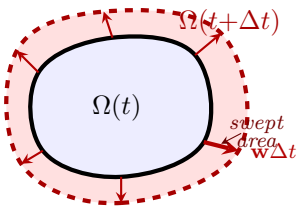

Figure 4: Temporal evolution of the control volume from $\Omega(t)$ (solid) to $\Omega(t+\Delta t)$ (dashed). The mesh velocity $\mathbf{w}$ varies along the boundary, producing a non-uniform expansion and deformation of the domain. The shaded region between the two boundaries represents the total swept volume over the interval Δt, which must equal the net volumetric flux $\int_{S(t)} \mathbf{w}\cdot\mathbf{n}\, dS\, \Delta t$ for the Geometric Conservation Law to be satisfied.

The first effect is the **local change**, wherein the field ϕ changes value at fixed points in space. This represents the internal evolution of the fluid properties independent of the grid's motion. The second effect is **boundary motion**, where the domain $\Omega(t)$ "sweeps" through space with a mesh velocity $\mathbf{w}$. As the boundaries move, the domain captures new fluid particles or leaves others behind, creating a volumetric flux that must be added to the internal rate of change.

This coupling between field evolution and geometric motion is formalized by the Leibniz integral rule for time-dependent volumes. It dictates that any change in $\mathcal{I}(t)$ is the sum of the integrated local temporal variation and the flux of the quantity ϕ across the moving surface. Establishing this relationship is the prerequisite for deriving the ALE-specific Reynolds Transport Theorem and ensuring that numerical schemes remain strictly conservative on deforming grids.

3.2 The Mapping and Pull-Back Strategy

To evaluate the time derivative of integrals defined over a deforming domain in a rigorous manner, it is convenient to reformulate the problem on a fixed reference configuration. This is achieved through a *pull-back* transformation, in which the time-dependent physical domain $\Omega(t)$ is mapped onto a static reference domain $\hat{\Omega}$, typically chosen as the initial configuration at $t = 0$. The mapping is defined by

$$\mathbf{x} = \boldsymbol{\chi}(\hat{\mathbf{x}}, t), \tag{20}$$

which establishes a one-to-one correspondence between referential coordinates $\hat{\mathbf{x}}$ and spatial coordinates $\mathbf{x}$.

Applying the change-of-variables theorem, the differential volume element transforms according to

$$d\Omega = J(\hat{\mathbf{x}}, t), d\hat{\Omega}, \tag{21}$$

where $J = \det(\mathbf{F})$ is the Jacobian associated with the deformation gradient $\mathbf{F} = \nabla_{\hat{\mathbf{x}}}\mathbf{x}$. This relation accounts for the local change in volume induced by the mapping.

As a result, the original integral over the moving domain can be rewritten entirely in the reference configuration as

$$\mathcal{I}(t) = \int_{\hat{\Omega}} \phi(\boldsymbol{\chi}(\hat{\mathbf{x}}, t), t), J(\hat{\mathbf{x}}, t), d\hat{\Omega}. \tag{22}$$

In this representation, all time dependence is contained within the integrand, while the domain of integration remains fixed.

This reformulation has a crucial consequence. Since the limits of integration are now independent of time, the time derivative can be taken inside the integral, yielding

$$\frac{d\mathcal{I}}{dt} = \int_{\hat{\Omega}} \frac{\partial}{\partial t}\Big[\phi(\boldsymbol{\chi}(\hat{\mathbf{x}}, t), t), J(\hat{\mathbf{x}}, t)\Big], d\hat{\Omega}. \tag{23}$$

This expression provides a mathematically consistent starting point for deriving conservation laws on deforming domains, as it separates the geometric complexity of the moving domain from the differentiation process.

3.3 Derivation of the Fundamental ALE Identity

Starting from the transformed integral in the reference configuration, the time derivative of the integrand involves the product of the field ϕ and the Jacobian J. Applying the product rule yields

$$\frac{\partial(\phi J)}{\partial t} = \left.\frac{\partial \phi}{\partial t}\right|_{\hat{\mathbf{x}}} J + \phi \left.\frac{\partial J}{\partial t}\right|_{\hat{\mathbf{x}}}. \tag{24}$$

This decomposition separates the contribution associated with the evolution of the field from that arising due to the geometric deformation of the domain.

3.3.1 Term A: The Referential Derivative

The first term, $\left.\frac{\partial \phi}{\partial t}\right|_{\hat{\mathbf{x}}}$, represents the rate of change of the field as observed while following a mesh point. Since the mesh moves with velocity $\mathbf{w} = \partial \boldsymbol{\chi}/\partial t$, this derivative is naturally expressed in terms of spatial quantities through the chain rule,

$$\left.\frac{\partial \phi}{\partial t}\right|_{\hat{\mathbf{x}}} = \frac{\partial \phi}{\partial t} + \mathbf{w} \cdot \nabla \phi. \tag{25}$$

This relation shows that the variation of ϕ along a mesh trajectory consists of two components: a local temporal change at a fixed spatial point and a transport contribution arising from the motion of the mesh through the spatial gradient of the field. The referential derivative therefore captures how the field is perceived in the moving computational frame.

3.3.2 Term B: Geometric Evolution

The second term involves the time evolution of the Jacobian, which reflects the geometric deformation of the mesh. A fundamental identity from continuum kinematics relates this quantity to the divergence of the mesh velocity,

$$\left.\frac{\partial J}{\partial t}\right|_{\hat{\mathbf{x}}} = J(\nabla \cdot \mathbf{w}). \tag{26}$$

This expression establishes that the rate of change of a differential volume element is governed by the local volumetric expansion or contraction of the mesh. When $\nabla \cdot \mathbf{w} > 0$, neighboring mesh points separate and the element expands; when $\nabla \cdot \mathbf{w} < 0$, the element contracts.

Together, these two contributions provide a complete description of how both the field and the underlying domain evolve in time, forming the basis for the fundamental ALE identity used in conservation laws.

3.4 The ALE Transport Identity

By substituting the expressions obtained for the two contributions in Equation 24 and factoring out the Jacobian, the time derivative of the integral can be written in the reference configuration as

$$\frac{d\mathcal{I}}{dt} = \int_{\hat{\Omega}} \left[\frac{\partial \phi}{\partial t} + \mathbf{w} \cdot \nabla \phi + \phi(\nabla \cdot \mathbf{w}) \right] J, d\hat{\Omega}. \tag{27}$$

This expression makes explicit the combined effect of the temporal variation of the field and the geometric evolution of the domain.

The terms involving the mesh velocity can be further simplified using the vector identity

$$\nabla \cdot (\phi \mathbf{w}) = \phi(\nabla \cdot \mathbf{w}) + \mathbf{w} \cdot \nabla \phi, \tag{28}$$

which allows the two contributions associated with mesh motion to be combined into a single divergence term. The integrand then takes a more compact and physically transparent form.

Finally, transforming the integral back to the physical domain using the relation $J, d\hat{\Omega} = d\Omega$, one obtains the *ALE transport identity*:

$$\frac{d}{dt} \int_{\Omega(t)} \phi, d\Omega = \int_{\Omega(t)} \left[\frac{\partial \phi}{\partial t} + \nabla \cdot (\phi \mathbf{w}) \right] d\Omega. \tag{29}$$

This identity provides the fundamental link between time derivatives over a deforming control volume and differential operators expressed in the spatial domain. It shows that the effect of mesh motion can be represented as an additional flux term, thereby preserving a conservative structure that is consistent with the underlying kinematics of the moving domain.

3.5 Significance for Numerical Conservation

The identity given in Equation 29 is purely geometric in nature and does not yet incorporate the specific physics governing the field ϕ. Its importance lies in the fact that it establishes a consistent kinematic framework for describing how integrals evolve over a deforming control volume. In particular, it reveals that the time variation of a quantity defined on a moving domain arises from two distinct mechanisms:

1. **Internal evolution:** the local temporal variation of the field, represented by the standard Eulerian time derivative,
2. **Geometric flux:** the transport of the field across the moving boundary $\partial\Omega(t)$ induced by the mesh velocity $\mathbf{w}$.

This decomposition provides a clear interpretation of how mesh motion contributes to the balance of conserved quantities. Even in the absence of physical transport, the motion of the control volume itself generates an apparent flux that must be accounted for in a consistent manner.

From a numerical standpoint, this result has direct and critical implications. It ensures that conservation laws for mass, momentum, and energy can be formulated correctly on a moving mesh, provided that the discretization accurately captures both the field evolution and the geometric changes of the domain. In particular, the mesh velocity $\mathbf{w}$ must be represented in a way that is consistent with the evolution of element volumes, as encoded by the Jacobian.

This requirement leads naturally to the Geometric Conservation Law (GCL), which enforces compatibility between mesh motion and volume change at the discrete level. The GCL is therefore not an additional physical principle, but a necessary condition for preserving the conservative structure of the governing equations when implemented on a deforming computational grid.

4 ALE Reynolds Transport Theorem

Within the ALE framework, conservation laws are expressed over a control volume $\Omega(t)$ whose geometry evolves in time according to the prescribed mesh motion. As a consequence, the formulation of balance equations requires a transport theorem that consistently accounts for both the temporal variation of the field variables and the motion of the domain itself.

In classical continuum mechanics, the Reynolds Transport Theorem (RTT) provides the necessary relation between the time derivative of an integral quantity and its local and flux contributions. However, the standard form of the theorem is derived under specific assumptions, typically corresponding either to fixed control volumes in the Eulerian description or to material volumes that move with the flow in the Lagrangian description.

The ALE framework generalizes this result by allowing the control volume to move with an arbitrary velocity $\mathbf{w}$, independent of the material velocity. This extension requires a reformulation of the transport theorem in which the relative motion between the material and the control volume is explicitly taken into account. The resulting ALE form of the Reynolds Transport Theorem provides the foundation for deriving conservation laws on deforming meshes in a manner that remains both consistent and conservative.

4.1 Statement of the ALE RTT

Let $\phi(\mathbf{x}, t)$ denote a sufficiently smooth scalar field defined over a time-dependent domain $\Omega(t)$ with boundary $\partial\Omega(t)$. The motion of the domain is characterized by a prescribed mesh (or grid) velocity field $\mathbf{w}(\mathbf{x}, t)$, which determines how the control volume evolves in time. In this setting, the Arbitrary Lagrangian–Eulerian (ALE) form of the Reynolds Transport Theorem provides

a rigorous relation between the time rate of change of an integral quantity and the kinematics of the moving domain.

The theorem is expressed as

$$\frac{d}{dt}\int_{\Omega(t)} \phi \, d\Omega = \int_{\Omega(t)} \frac{\partial \phi}{\partial t} \, d\Omega + \int_{\partial\Omega(t)} \phi \, \mathbf{w} \cdot \mathbf{n} \, dS. \tag{30}$$

This identity decomposes the total time derivative of the integral into two distinct and physically interpretable contributions. The first term represents the local, pointwise rate of change of the scalar field at fixed spatial coordinates. It captures intrinsic temporal variations of ϕ that would be observed even if the domain were stationary. The second term accounts for the transport of ϕ induced purely by the motion of the control volume boundary. Specifically, the normal component of the mesh velocity, $\mathbf{w} \cdot \mathbf{n}$, determines whether material is effectively entering or leaving the domain due to boundary deformation or displacement.

This separation is fundamental in the ALE framework. It distinguishes between changes caused by the evolution of the field itself and those arising from the kinematics of the computational domain. As a result, the theorem provides the essential bridge between integral conservation laws and their formulation on moving meshes, enabling consistent treatment of deforming geometries without committing to a purely Lagrangian or purely Eulerian description.

4.2 Divergence Form

To facilitate a purely volumetric description of the transport process, the Reynolds Transport Theorem (RTT) is reformulated by converting the boundary integral into a volume integral. This transformation is essential for developing finite volume or finite element schemes where the conservation laws are enforced over a control volume $\Omega(t)$. By applying the Gauss divergence theorem, the flux across the moving boundary $\partial\Omega(t)$ due to the mesh velocity $\mathbf{w}$ is expressed as:

$$\int_{\partial\Omega(t)} \phi \, \mathbf{w} \cdot \mathbf{n} \, dS = \int_{\Omega(t)} \nabla \cdot (\phi \mathbf{w}) \, d\Omega. \tag{31}$$

The integrand $\nabla \cdot (\phi \mathbf{w})$ represents the spatial variation of the field ϕ as it is transported by the moving mesh. To better understand the interaction between the field and the mesh motion, the divergence of the product is expanded using the standard vector identity:

$$\nabla \cdot (\phi \mathbf{w}) = \mathbf{w} \cdot \nabla \phi + \phi \, \nabla \cdot \mathbf{w}. \tag{32}$$

In this expansion, the term $\mathbf{w} \cdot \nabla \phi$ represents the advection of the property ϕ relative to the mesh, while $\phi \, \nabla \cdot \mathbf{w}$ accounts for the change in the local density of ϕ due to the dilatation or contraction of the control volume itself. Substituting this expanded form into the RTT yields an expression that combines the local Eulerian time derivative with the transport terms:

$$\frac{d}{dt}\int_{\Omega(t)} \phi \, d\Omega = \int_{\Omega(t)} \left(\frac{\partial \phi}{\partial t} + \mathbf{w} \cdot \nabla \phi + \phi \, \nabla \cdot \mathbf{w} \right) d\Omega. \tag{33}$$

The first two terms within the integrand, $\frac{\partial \phi}{\partial t} + \mathbf{w} \cdot \nabla \phi$, constitute the definition of the referential time derivative, denoted as $\left.\frac{\partial \phi}{\partial t}\right|_{\hat{\mathbf{x}}}$. This derivative quantifies the rate of change of the field ϕ as observed from a coordinate $\hat{\mathbf{x}}$ that is fixed in the referential (mesh) domain. By invoking this relationship, the transport theorem is cast into the compact ALE divergence form:

$$\frac{d}{dt}\int_{\Omega(t)} \phi \, d\Omega = \int_{\Omega(t)} \left(\left.\frac{\partial \phi}{\partial t}\right|_{\hat{\mathbf{x}}} + \phi \, \nabla \cdot \mathbf{w} \right) d\Omega. \tag{34}$$

This final expression clarifies that the total rate of change of the integrated quantity is a result of both the intrinsic change of the field at a referential point and the volumetric scaling induced by the divergence of the mesh velocity field.

4.3 Connection to the Jacobian

The transition from a moving spatial domain $\Omega(t)$ to a fixed referential domain $\hat{\Omega}$ is formally established through a kinematic mapping $\mathbf{x} = \boldsymbol{\chi}(\hat{\mathbf{x}}, t)$. This mapping, assumed to be a diffeomorphism, allows for the transformation of integrals by introducing the Jacobian $J(\hat{\mathbf{x}}, t) = \det(\partial \mathbf{x}/\partial \hat{\mathbf{x}})$, which represents the ratio of a differential volume element in the physical configuration to its counterpart in the referential configuration ($d\Omega = J\, d\hat{\Omega}$). Consequently, the integral of a scalar field ϕ over the time-varying domain is expressed as:

$$\int_{\Omega(t)} \phi(\mathbf{x}, t)\, d\Omega = \int_{\hat{\Omega}} \phi(\boldsymbol{\chi}(\hat{\mathbf{x}}, t), t)\, J(\hat{\mathbf{x}}, t)\, d\hat{\Omega}. \tag{35}$$

A primary advantage of this referential description is that the domain $\hat{\Omega}$ is by definition time-invariant. This allows the material time derivative to commute with the integral sign. Applying the product rule to the integrand on the referential domain yields:

$$\frac{d}{dt} \int_{\Omega(t)} \phi\, d\Omega = \int_{\hat{\Omega}} \left[\left. \frac{\partial \phi}{\partial t} \right|_{\hat{\mathbf{x}}} J + \phi \left. \frac{\partial J}{\partial t} \right|_{\hat{\mathbf{x}}} \right] d\hat{\Omega}. \tag{36}$$

To resolve the temporal evolution of the Jacobian, we invoke Euler's expansion formula, which relates the rate of change of the volume ratio to the divergence of the mesh velocity $\mathbf{w} = \partial \boldsymbol{\chi}/\partial t|_{\hat{\mathbf{x}}}$. Specifically, the identity:

$$\left. \frac{\partial J}{\partial t} \right|_{\hat{\mathbf{x}}} = J(\nabla \cdot \mathbf{w}), \tag{37}$$

quantifies how the local volume scales in response to the mesh motion. Substituting this kinematic relationship into the integral expression leads to a consolidated form on the referential domain:

$$\frac{d}{dt} \int_{\Omega(t)} \phi\, d\Omega = \int_{\hat{\Omega}} \left[J \left(\left. \frac{\partial \phi}{\partial t} \right|_{\hat{\mathbf{x}}} + \phi \nabla \cdot \mathbf{w} \right) \right] d\hat{\Omega}. \tag{38}$$

Mapping this result back to the physical domain $\Omega(t)$ by substituting $d\hat{\Omega} = J^{-1} d\Omega$ recovers the ALE Reynolds Transport Theorem. This derivation underscores a critical requirement for numerical stability: the mapping $\boldsymbol{\chi}$ must remain non-singular ($J > 0$) throughout the simulation. If the mesh motion leads to excessive distortion or inversion ($J \leq 0$), the kinematic consistency of the ALE formulation is lost, necessitating remeshing or regularization of the mesh velocity field $\mathbf{w}$.

4.4 Consistency with Classical Limits

The mathematical robustness of the Arbitrary Lagrangian-Eulerian (ALE) formulation is fundamentally rooted in its status as a generalized kinematic framework. By treating the mesh velocity $\mathbf{w}$ as an independent kinematic variable, the ALE description allows for a continuous transition between the spatial (Eulerian) and material (Lagrangian) frames of reference. This flexibility ensures that the ALE Reynolds Transport Theorem (RTT) remains consistent with classical continuum mechanics, recovering the standard transport equations as limiting cases of the mesh motion.

The Eulerian limit is recovered when the mesh velocity is constrained to be zero ($\mathbf{w} = \mathbf{0}$), implying that the referential domain remains stationary and coincident with the physical domain for all $t > 0$. In this scenario, the control volume Ω is fixed in space, and the volumetric expansion term $\phi \nabla \cdot \mathbf{w}$ vanishes. Furthermore, because there is no relative motion between the mesh and the spatial coordinates, the referential time derivative $\partial \phi/\partial t|_{\hat{\mathbf{x}}}$ becomes identical to

the local Eulerian time derivative $\partial\phi/\partial t$. Under these conditions, the ALE RTT simplifies to the classical Eulerian expression:

$$\frac{d}{dt}\int_{\Omega}\phi\,d\Omega = \int_{\Omega}\frac{\partial\phi}{\partial t}\,d\Omega. \tag{39}$$

This description is computationally efficient for fluid flows in rigid, non-deforming geometries, though it requires specialized interface-capturing methods to resolve moving boundaries or free surfaces.

In contrast, the Lagrangian limit is attained when the mesh velocity is set equal to the material velocity of the fluid ($\mathbf{w} = \mathbf{v}$). Here, the mesh points are no longer stationary relative to the fluid but instead track individual material particles. In this regime, the referential domain $\hat{\Omega}$ is equivalent to the initial material configuration, and the combination of the local rate of change and the convective term constitutes the material derivative $D\phi/Dt$. Consequently, the ALE transport equation reduces to:

$$\frac{d}{dt}\int_{\Omega(t)}\phi\,d\Omega = \int_{\Omega(t)}\frac{D\phi}{Dt}\,d\Omega, \tag{40}$$

where $\Omega(t)$ denotes a material volume. While the Lagrangian description is naturally suited for identifying material boundaries and preserving history-dependent properties, its applicability in fluid dynamics is often limited by severe mesh distortion in regions of high shear or vorticity. By maintaining a mesh velocity $\mathbf{w}$ that is distinct from both $\mathbf{0}$ and $\mathbf{v}$, the ALE method provides a consistent generalization that mitigates the convective errors of the Eulerian approach while avoiding the topological degradation characteristic of the Lagrangian approach.

4.5 Physical Interpretation

The ALE Reynolds Transport Theorem (RTT) provides a fundamental kinematic decomposition, separating the total rate of change of an integrated quantity into two distinct physical mechanisms. This separation is critical for maintaining the conservative properties of a numerical scheme when the underlying computational grid is subject to motion and deformation. As illustrated in Figure 5, the interaction between the material flow and the grid geometry determines the net transport.

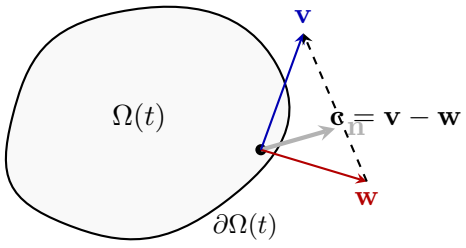

Figure 5: Kinematic interaction at the boundary $\partial\Omega(t)$. While $\mathbf{v}$ and $\mathbf{w}$ describe material and mesh motion respectively, only the normal component of the relative velocity $\mathbf{c}$ drives the physical flux across the moving interface.

By analyzing the integrand in the compact ALE divergence form, the total variation is partitioned into a temporal component and a geometric component. The first mechanism is the **temporal variation observed on the moving mesh**, represented by the referential time derivative $\partial\phi/\partial t|_{\hat{\mathbf{x}}}$. This term quantifies the rate at which the quantity ϕ changes at a fixed coordinate in the referential domain. Physically, this corresponds to the "internal" change of the field as perceived by an observer moving synchronously with the mesh node. In a numerical

context, the mesh effectively "carries" the information, updating the value based on local physics while its spatial position evolves.

The second mechanism is the **geometric variation**, represented by the product $\phi \nabla \cdot \mathbf{w}$. This term is purely kinematic and accounts for the expansion or contraction of the control volume $\Omega(t)$. As seen in Figure 5, the mesh velocity $\mathbf{w}$ acts upon the boundary $\partial\Omega(t)$ with outward normal $\mathbf{n}$. The divergence $\nabla \cdot \mathbf{w}$ represents the volumetric manifestation of this boundary motion, i.e. the swept-volume effect. Physically, if the mesh is expanding ($\nabla \cdot \mathbf{w} > 0$), the volume of the control element increases, which would decrease the concentration of ϕ per unit volume if the total amount were fixed. Conversely, a contracting mesh ($\nabla \cdot \mathbf{w} < 0$) concentrates the quantity.

The explicit separation of these terms is essential for ensuring that the conservation laws remain physically consistent. Without the geometric contribution, a numerical solver would fail to distinguish between a physical increase in the quantity ϕ and an apparent increase caused by the shrinking of the underlying mesh cells. This ensures that the integral value is adjusted for the changing metric of the domain, a requirement formally codified in the **Geometric Conservation Law (GCL)**. However, a significant limitation of this decomposition arises in the presence of extreme mesh distortion; if the mesh velocity field $\mathbf{w}$ lacks sufficient smoothness, the $\nabla \cdot \mathbf{w}$ term may introduce numerical oscillations or lead to non-physical "shocks" in the Jacobian distribution, emphasizing the need for robust mesh regularization techniques in ALE-based simulations.

5 Governing Equations in ALE Form

The application of the ALE framework to the Navier-Stokes equations necessitates a consistent transformation of the convective transport terms. Unlike the classical Eulerian formulation, where transport is governed solely by the material velocity $\mathbf{v}$, the ALE description introduces a relative velocity (or convective velocity) defined as $\mathbf{c} = \mathbf{v} - \mathbf{w}$. This velocity represents the rate at which fluid crosses the moving boundaries of the control volumes, effectively decoupling the physical flow from the underlying discretization. The key mathematical shifts required to transition from a fixed to a moving frame are summarized in Table 2.

Table 2: Comparison of fundamental operators and terms in Standard Eulerian and ALE formulations.

Term	**Standard Eulerian**	**ALE Form**
Time Derivative	$\dfrac{\partial}{\partial t}$	$\left.\dfrac{\partial}{\partial t}\right\|_{\hat{\mathbf{x}}}$
Convection	$\mathbf{v} \cdot \nabla(\cdot)$	$(\mathbf{v} - \mathbf{w}) \cdot \nabla(\cdot)$
Incompressibility	$\nabla \cdot \mathbf{v} = 0$	$\nabla \cdot \mathbf{v} = 0$
Mass flux	$\nabla \cdot (\rho \mathbf{v})$	$\nabla \cdot \big[\rho(\mathbf{v} - \mathbf{w})\big]$
Momentum flux	$\nabla \cdot (\rho \mathbf{v} \otimes \mathbf{v})$	$\nabla \cdot \big[\rho \mathbf{v} \otimes (\mathbf{v} - \mathbf{w})\big]$
Energy flux	$\nabla \cdot (E \mathbf{v})$	$\nabla \cdot \big[E(\mathbf{v} - \mathbf{w})\big]$
Mesh Speed	$\mathbf{w} = \mathbf{0}$	$\mathbf{w}$ (arbitrary)

As the comparison shows, the key modification appears in the convective flux: the material velocity $\mathbf{v}$ is replaced by the relative velocity $\mathbf{c} = \mathbf{v} - \mathbf{w}$ in the transport term of every conservation law (mass, momentum, and energy). This ensures that advective transport is attributed only to the motion of the fluid relative to the grid, regardless of how the grid itself

moves. The incompressibility constraint $\nabla \cdot \mathbf{v} = 0$ remains invariant across frames because it is an intrinsic constraint on the material's volumetric behaviour, independent of the kinematic description of the mesh. The following subsections apply these principles to the conservation of mass, momentum, and energy, and examine how the mesh motion $\mathbf{w}$ enters each equation.

5.1 Mass Conservation

The principle of mass conservation dictates that the total mass within a material volume remains invariant. In the ALE framework, this global conservation law is mapped onto a time-deforming control volume $\Omega(t)$. By substituting the fluid density ρ for the general scalar field ϕ in the ALE Reynolds Transport Theorem, we derive the strong form of the continuity equation. Depending on the choice of mathematical arrangement, this leads to two primary representations: the convective form and the divergence (conservative) form.

The convective form is obtained by expressing the rate of change relative to the referential coordinate $\hat{\mathbf{x}}$. In this configuration, the local change in density is coupled with the transport of mass due to the relative velocity $\mathbf{c} = \mathbf{v} - \mathbf{w}$ and the intrinsic expansion of the fluid:

$$\left.\frac{\partial \rho}{\partial t}\right|_{\hat{\mathbf{x}}} + (\mathbf{v} - \mathbf{w}) \cdot \nabla \rho + \rho \nabla \cdot \mathbf{v} = 0. \tag{41}$$

This formulation highlights the kinematic competition between the material velocity $\mathbf{v}$ and the mesh velocity $\mathbf{w}$. When $\mathbf{w}$ is strategically chosen to follow the fluid motion, the convective term $(\mathbf{v} - \mathbf{w}) \cdot \nabla \rho$ is minimized, thereby reducing the numerical errors associated with the discretization of high-gradient transport.

Alternatively, the equation can be cast into a divergence form, which is preferred for numerical schemes where strict conservation at the discrete level is required:

$$\frac{\partial \rho}{\partial t} + \nabla \cdot (\rho(\mathbf{v} - \mathbf{w})) + \rho \nabla \cdot \mathbf{w} = 0. \tag{42}$$

In this expression, the term $\nabla \cdot (\rho(\mathbf{v} - \mathbf{w}))$ represents the net mass flux across the moving boundary of the control volume. The second term, $\rho \nabla \cdot \mathbf{w}$, represents a purely geometric source term that accounts for the variation in the density field induced by the dilatation or contraction of the mesh cells.

This decomposition reveals a critical requirement for ALE-based solvers: the numerical integration of the mass flux and the geometric term must be synchronized to prevent the generation of non-physical mass sources or sinks. While the total mass remains theoretically invariant regardless of the mesh velocity field, a poorly regularized $\mathbf{w}$ can lead to excessive numerical diffusion or dispersion. In the limit of high-speed flows or significant mesh distortion, the accuracy of the mass conservation is often limited by the degree to which the mesh motion satisfies the Geometric Conservation Law (GCL), which ensures that a constant density field can be exactly preserved on a deforming grid.

5.2 Incompressible Limit

In the limit of incompressible flow, the fluid density ρ is assumed to be spatially uniform and temporally invariant. Within the ALE framework, this assumption imposes a strict kinematic constraint on the material velocity field $\mathbf{v}$ that remains independent of the arbitrary motion of the mesh $\mathbf{w}$. When the condition $\rho = \text{const.}$ is applied to the ALE mass conservation equation, the local time derivative and the density gradients vanish, reducing the continuity requirement to the statement that the material velocity field must be solenoidal:

$$\nabla \cdot \mathbf{v} = 0. \tag{43}$$

This isochoric constraint implies that while the computational control volumes $\Omega(t)$ may undergo significant dilatation or contraction due to the mesh velocity field $\mathbf{w}$, the net volumetric flux of the fluid across these moving boundaries must exactly balance the rate of change of the control volume itself. Consequently, the divergence-free condition on $\mathbf{v}$ ensures that the fluid particles do not undergo any change in volume, regardless of how the underlying discretization deforms to accommodate boundary motion or interface tracking.

From a numerical perspective, the enforcement of $\nabla \cdot \mathbf{v} = 0$ ensures that the pressure-velocity coupling remains formally analogous to a classical Eulerian formulation. In most ALE solvers, this is achieved by solving a pressure Poisson equation or utilizing a projection method to satisfy the solenoidal constraint at each time step. However, a critical requirement for maintaining accuracy on deforming grids is the adherence to the Discrete Geometric Conservation Law (DGCL). The DGCL dictates that a constant density field must be preserved exactly, even as the mesh undergoes arbitrary motion. If the numerical schemes for the convective flux and the mesh volume change are not temporally synchronized, the solver may introduce spurious source terms into the continuity equation. These errors typically manifest as non-physical pressure oscillations or "spurious waves," which can compromise the stability of the simulation. Thus, in the ALE context, the incompressible limit requires not only a divergence-free material velocity but also a discrete kinematic mapping that ensures the geometric integrity of the moving control volumes.

5.3 Momentum Conservation

The conservation of linear momentum within the ALE framework is established by applying the Reynolds Transport Theorem to the momentum density $\rho\mathbf{v}$ over a time-deforming control volume $\Omega(t)$. By transforming the material time derivative into its referential counterpart, the momentum equation for a Newtonian fluid is cast into a form that explicitly accounts for the mesh motion $\mathbf{w}$. The resulting strong form of the ALE momentum equation in convective (non-conservative) form is given by:

$$\rho \left(\left. \frac{\partial \mathbf{v}}{\partial t} \right|_{\hat{\mathbf{x}}} + (\mathbf{v} - \mathbf{w}) \cdot \nabla \mathbf{v} \right) = -\nabla p + \mu \Delta \mathbf{v} + \rho \mathbf{f}. \tag{44}$$

The term $(\mathbf{v}-\mathbf{w}) \cdot \nabla \mathbf{v}$ represents the ALE convective acceleration, where the effective transport of momentum is governed not by the material velocity $\mathbf{v}$ alone, but by the relative (or advective) velocity $\mathbf{c} = \mathbf{v} - \mathbf{w}$. This modification is the cornerstone of the ALE method's versatility. In the Lagrangian limit ($\mathbf{w} = \mathbf{v}$), the convective velocity vanishes, and the equation simplifies to a purely inertial balance observed from a material point. Conversely, in the Eulerian limit ($\mathbf{w} = \mathbf{0}$), the standard spatial convection is recovered.

For incompressible flow, the divergence-free condition $\nabla \cdot \mathbf{v} = 0$ allows an equivalent *conservative* (divergence) form to be derived by combining the momentum and continuity equations:

$$\left. \frac{\partial (\rho \mathbf{v})}{\partial t} \right|_{\hat{\mathbf{x}}} + \nabla \cdot \left[\rho \mathbf{v} \otimes (\mathbf{v} - \mathbf{w}) \right] = -\nabla p + \nabla \cdot \boldsymbol{\sigma} + \rho \mathbf{f}, \tag{45}$$

where $\boldsymbol{\sigma} = \mu(\nabla \mathbf{v} + \nabla \mathbf{v}^T)$ is the viscous stress tensor. This form is preferred in finite volume methods because the divergence structure ensures exact conservation of momentum across cell faces: the flux of $\rho\mathbf{v}$ leaving one cell equals the flux entering its neighbour, which is important for overall momentum balance and for capturing sharp flow features. The convective form (44) and the conservative form (45) are analytically equivalent under $\nabla \cdot \mathbf{v} = 0$, but may differ at the discrete level when the incompressibility constraint is only approximately satisfied.

The pressure gradient ∇p, the viscous stress, and the body forces $\rho\mathbf{f}$ on the right-hand side remain identical to those of the classical Eulerian Navier–Stokes equations. This is because these terms represent physical stresses and external forces that depend on the instantaneous

spatial configuration of the fluid rather than the choice of the referential coordinate system. However, the numerical discretization of these terms requires care: the spatial operators must be evaluated on the deformed geometry at each time step, which necessitates a mapping that preserves the second-order accuracy of the viscous stresses despite potential mesh distortion.

From a computational standpoint, the ALE formulation offers a distinct advantage regarding numerical stability. The stability of explicit or semi-implicit time-integration schemes is governed by the Courant–Friedrichs–Lewy (CFL) condition, which in the ALE context reads

$$\Delta t \;\leq\; \min_i \frac{h_i}{|\mathbf{c}_i|} = \min_i \frac{h_i}{|\mathbf{v}_i - \mathbf{w}_i|}, \tag{46}$$

where h_i is the local mesh spacing at node i. By prescribing $\mathbf{w}$ so that the mesh follows the bulk flow, the magnitude of the relative velocity $|\mathbf{c}|$ is reduced, which directly relaxes the time-step constraint compared to a fixed Eulerian grid. Nevertheless, this advantage is bounded by the need to maintain mesh quality; a mesh velocity field that minimizes the CFL constraint but leads to high mesh skewness will ultimately degrade the accuracy of the gradient approximations and may lead to non-physical solutions or solver divergence.

5.4 Energy Conservation

The set of ALE conservation laws is completed by the energy equation, which governs the transport of total energy within the moving control volume. For a compressible Newtonian fluid, the total energy per unit volume is $E = \rho e + \frac{1}{2}\rho|\mathbf{v}|^2$, where e denotes the specific internal energy. Applying the ALE Reynolds Transport Theorem to E and invoking the divergence theorem for the pressure and viscous work terms yields the strong form of the ALE energy equation:

$$\left.\frac{\partial E}{\partial t}\right|_{\hat{\mathbf{x}}} + \nabla \cdot \left[E\,(\mathbf{v} - \mathbf{w})\right] = -\nabla \cdot (p\mathbf{v}) + \nabla \cdot (\boldsymbol{\tau} \cdot \mathbf{v}) - \nabla \cdot \mathbf{q} + \rho\,\mathbf{f} \cdot \mathbf{v}, \tag{47}$$

where $\boldsymbol{\tau} = \mu(\nabla\mathbf{v} + \nabla\mathbf{v}^T) - \frac{2}{3}\mu(\nabla \cdot \mathbf{v})\mathbf{I}$ is the viscous stress tensor and $\mathbf{q}$ is the heat flux vector, typically modeled by Fourier's law as $\mathbf{q} = -k\nabla T$. As in the mass and momentum equations, the sole modification introduced by the ALE framework is the replacement of the material velocity $\mathbf{v}$ with the convective velocity $\mathbf{v} - \mathbf{w}$ in the transport flux, while all source and diffusive terms retain their standard Eulerian forms evaluated on the instantaneous configuration $\Omega(t)$.

In the practically important limit of *incompressible flow* with negligible viscous dissipation, the energy equation decouples from mass and momentum and reduces to a scalar advection–diffusion equation for the temperature T:

$$\rho c_p \left[\left.\frac{\partial T}{\partial t}\right|_{\hat{\mathbf{x}}} + (\mathbf{v} - \mathbf{w}) \cdot \nabla T\right] = \nabla \cdot (k\nabla T) + \dot{q}, \tag{48}$$

where c_p is the specific heat at constant pressure and $\dot{q}$ is an internal heat source. The structure mirrors the ALE momentum equation: the referential time derivative tracks the thermal state along the mesh trajectory, while the relative convective velocity $\mathbf{v} - \mathbf{w}$ governs the transport of thermal energy across the moving control volume boundaries. This reflects the central principle of the ALE framework: every conserved scalar or vector quantity obeys the same kinematic substitution $\mathbf{v} \to \mathbf{v} - \mathbf{w}$ in its convective flux, with no change to the diffusive or source terms. As a result, any existing solver for standard Eulerian thermal or species transport can be extended to the ALE framework by replacing the advective velocity with the relative velocity, provided the temporal discretization is also updated to enforce the Geometric Conservation Law.

6 Geometric Conservation Law (GCL)

The integrity of an ALE-based simulation depends fundamentally on the synchronization between the numerical integration of the conservation laws and the temporal evolution of the computational grid. While the ALE Reynolds Transport Theorem provides the mathematical framework for transport on moving meshes, its discrete implementation must satisfy the Geometric Conservation Law (GCL) [Lesoinne and Farhat, 1996]. The GCL is a consistency requirement which dictates that the numerical scheme must be capable of exactly preserving a uniform constant field (such as a constant density or pressure) regardless of the magnitude or complexity of the mesh motion.

Physically, the GCL ensures that the change in the volume of a control element is exactly accounted for by the integrated motion of its boundaries. If the discrete approximation of the mesh velocity $\mathbf{w}$ does not perfectly match the rate of change of the cell volume, the solver will perceive the mesh deformation as a physical source or sink of the transported quantity. This section examines the GCL in both its continuous differential form and its discrete algorithmic representation, highlighting why its satisfaction is a prerequisite for the stability and conservation of any ALE solver.

6.1 Continuous Form

In the continuous limit, the Geometric Conservation Law (GCL) is a differential expression that relates the temporal evolution of the mapping's metric to the velocity field of the mesh. At any point in the referential domain, the Jacobian J serves as the local measure of volumetric deformation. For the ALE formulation to be kinematically consistent, the rate of change of this volume ratio must be exactly balanced by the divergence of the mesh velocity $\mathbf{w}$. This relationship is formally expressed by the identity:

$$\frac{\partial J}{\partial t} + \nabla \cdot (J\mathbf{w}) = 0 \tag{49}$$

Physically, this equation represents the conservation of volume in the mapping between the referential and spatial configurations. It ensures that the time-varying spatial domain $\Omega(t)$ is tracked continuously without the inadvertent creation or destruction of space within the computational grid.

From a mathematical standpoint, this continuous form is an extension of Euler's expansion formula, which states that $\partial J/\partial t|_{\hat{\mathbf{x}}} = J(\nabla \cdot \mathbf{w})$. By casting this identity into a conservation form, we emphasize that any local change in the mesh density, represented by J, must be accounted for by the flux of the mesh coordinates themselves. Dividing through by $J > 0$, the GCL can equivalently be written in the normalized form:

$$\frac{1}{J}\frac{\partial J}{\partial t} = \nabla \cdot \mathbf{w}, \tag{50}$$

which directly states that the volumetric rate of expansion of a mesh cell equals the divergence of the mesh velocity field. Satisfying this differential identity is a necessary condition for the ALE Reynolds Transport Theorem to recover a constant field; if the mesh moves but the Jacobian does not evolve in strict accordance with $\nabla \cdot \mathbf{w}$, the resulting numerical solution will be contaminated by artificial gradients that do not exist in the physical system.

A practical test of whether a code satisfies the GCL is the *freestream preservation* check: one plugs a perfectly uniform, steady flow ($\rho = \text{const}$, $\mathbf{v} = \text{const}$, $p = \text{const}$) into the ALE mass conservation equation and verifies that it is satisfied identically. Substituting into the compressible ALE continuity equation yields

$$\frac{\partial \rho}{\partial t} + \rho \nabla \cdot \mathbf{v} - \rho \nabla \cdot \mathbf{w} + (\mathbf{v} - \mathbf{w}) \cdot \nabla \rho = 0. \tag{51}$$

For the constant-field state, all density gradients and physical-flow divergence terms vanish, leaving the residual condition

$$\rho\left(\nabla \cdot \mathbf{w}\right) = 0. \tag{52}$$

Since $\rho \neq 0$, this requires $\nabla \cdot \mathbf{w} = 0$ at every point wherever the mesh is not expanding. On a deforming grid this condition is only satisfied if the temporal evolution of the Jacobian exactly balances the mesh velocity divergence, i.e. the GCL holds. Any scheme that fails this freestream preservation test will introduce non-physical sources even in the complete absence of physical gradients.

6.2 Discrete Form

The transition from a continuous differential identity to a computational framework necessitates the formulation of the Discrete Geometric Conservation Law (DGCL) [Farhat et al., 2001]. In a finite volume context, the DGCL ensures that the temporal evolution of a cell volume V is perfectly synchronized with the integrated motion of its bounding surfaces. For a control volume transitioning from time level n to $n+1$ over a discrete time increment Δt, the conservation of volume is expressed through the following identity:

$$\frac{V^{n+1} - V^n}{\Delta t} = \sum_f \mathbf{w}_f \cdot \mathbf{n}_f A_f. \tag{53}$$

In this expression, V^{n+1} and V^n represent the measures of the cell volume at the respective time levels, while the summation index f iterates over the set of faces bounding the cell. The term $\mathbf{w}_f \cdot \mathbf{n}_f A_f$ denotes the volumetric flux across a face, where $\mathbf{w}_f$ is the mesh velocity at the face center, $\mathbf{n}_f$ is the outward-pointing unit normal, and A_f is the face area. This relationship is conceptually grounded in the "swept volume" principle, as illustrated in Figure 6.

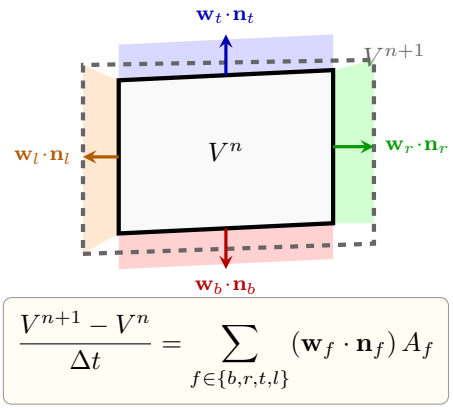

Figure 6: Illustration of the Discrete Geometric Conservation Law (DGCL) for a two-dimensional control volume. The cell transitions from V^n (solid) to V^{n+1} (dashed), with each of the four faces displaced at a different mesh velocity $\mathbf{w}_f$. The coloured swept regions represent the volume contribution of each face; their sum must identically equal $V^{n+1} - V^n$ for the DGCL to hold. Any inconsistency between the discrete volume update and the face-swept volumes introduces a spurious algebraic source into the conservation equations, independently of mesh quality or time-step size.

The physical significance of the DGCL lies in ensuring that the right-hand side of the equation, representing the total volume generated by the displacement of the cell boundaries, is identically equal to the net change in the cell's storage capacity. If this identity is not satisfied, the numerical solver will inadvertently introduce artificial mass or momentum sources into the governing equations, even in the absence of physical gradients. Such "geometric residuals"

are a common source of instability in moving-mesh simulations, particularly in high-speed or incompressible flows where the pressure field is highly sensitive to volumetric errors.

A critical implication for algorithm design is that the time-integration scheme used for the mesh motion must be strictly compatible with the scheme used for the fluid transport. For instance, if the cell volume V^{n+1} is calculated based on the updated coordinates of the vertices, the mesh velocity $\mathbf{w}_f$ and the face areas A_f must be evaluated using a quadrature rule or averaging technique that exactly recovers the volume change. Failure to achieve this algorithmic coupling, often due to inconsistent temporal orders for the geometric and kinematic updates, results in a violation of the DGCL, contaminating the solution with non-physical errors that can jeopardize the overall convergence of the ALE framework.

6.3 Importance

The significance of the Geometric Conservation Law (GCL) transcends mere numerical refinement; it is a fundamental requirement for the consistency and stability of any ALE-based discretization. The primary metric for evaluating the GCL is the principle of *freestream preservation*, which dictates that a numerical scheme must exactly maintain a uniform constant state (such as a constant pressure and velocity field) regardless of the magnitude or complexity of the mesh deformation. The failure to satisfy the GCL leads to several critical numerical pathologies that can compromise the validity of the entire computational model.

First, a violation of the GCL introduces spurious source terms into the discrete conservation equations. These artificial sources arise because the numerical approximation of the mesh's volumetric change ($\partial J/\partial t$) does not perfectly cancel the discrete divergence of the mesh velocity ($\nabla \cdot \mathbf{w}$). Consequently, even in a physically quiescent flow, the solver perceives the mesh motion as a local creation or destruction of mass and momentum. These non-physical "geometric" residuals act as stochastic noise that contaminates the solution, often manifesting as high-frequency oscillations that obscure the underlying physics.

Second, these spurious terms frequently lead to numerical instability, particularly in incompressible or low-Mach number flows where the pressure-velocity coupling is highly sensitive to mass-flux consistency. In such cases, the artificial mass sources generated by GCL violations trigger erratic pressure fluctuations. These fluctuations, in turn, drive non-physical velocity gradients, creating a feedback loop that can lead to solver divergence. This instability is often difficult to mitigate through standard temporal or spatial refinement alone, as it is rooted in the lack of kinematic synchronization between the mesh update and the transport operators.

Finally, the absence of GCL compliance results in the loss of global conservation. Since the total integral of a conserved quantity over the domain is no longer invariant under arbitrary mesh motion, the simulation may exhibit a temporal drift in total mass or energy. This loss of conservation is particularly detrimental in long-duration simulations or in fluid-structure interaction (FSI) problems, where the accumulation of geometric errors at the moving interface can lead to unphysical energy transfer between the fluid and the solid. Satisfying the GCL is therefore a prerequisite for the reliability of the ALE framework; it is typically achieved by employing a temporal integration scheme that treats the mesh velocity and the control volume change with consistent quadrature.

7 Numerical Formulations

The numerical realization of the ALE equations involves the translation of the continuous kinematic identities into a discrete algebraic system where the spatial metric is no longer invariant. This transition requires a discretization scheme that can simultaneously account for the fluid-mesh relative transport and the geometric evolution of the underlying computational grid. Whether employing the variational framework of the Finite Element Method or the integral bal-

ance approach of the Finite Volume Method, the solver must ensure that the discrete operators for convection and diffusion are consistently updated to reflect the instantaneous configuration of the domain. This section outlines the fundamental numerical architectures used to solve the ALE-formulated Navier-Stokes equations, emphasizing the calculation of numerical fluxes and the temporal synchronization required to satisfy the Geometric Conservation Law.

7.1 Finite Element Method (FEM)

The implementation of the ALE framework within the Finite Element Method (FEM) is predicated on a variational approach where the governing equations are integrated over the time-varying spatial domain $\Omega(t)$ [Donea and Huerta, 2003, Donea et al., 2004]. Unlike standard Eulerian FEM, where the mesh is static, the ALE-FEM formulation requires the trial and test functions to be defined via a time-dependent mapping from a fixed referential domain $\hat{\Omega}$. This results in the use of "moving" test functions that are stationary in the referential frame but implicitly time-dependent in the spatial frame. Consequently, the referential time derivative $\partial\phi/\partial t|_{\hat{\mathbf{x}}}$ can be computed by differentiating the nodal coefficients directly, as the basis functions effectively follow the trajectory of the mesh points. This kinematic synchronization ensures that the discrete transport terms naturally account for the relative motion between the fluid and the grid.

For incompressible flows, the spatial discretization of the velocity and pressure fields must satisfy the Ladyzhenskaya-Babuška-Brezzi (LBB), or inf-sup, stability condition. This condition is a fundamental requirement to ensure that the pressure is uniquely determined and free of spurious numerical modes, such as the checkerboard effect. In the context of ALE, the LBB condition remains a critical constraint; however, the evolving geometry introduces additional complexity. As the mesh deforms, the inf-sup constant, which dictates the stability margin of the mixed formulation, may degrade due to element distortion. Severe mesh skewness or high aspect ratios can weaken the coupling between the velocity and pressure spaces, potentially leading to instability even if the element pair (e.g., Taylor-Hood) is theoretically stable on an undistorted grid.

To mitigate these risks, ALE-FEM implementations commonly rely on two complementary Petrov-Galerkin stabilization techniques. The first is the *Streamline Upwind/Petrov-Galerkin* (SUPG) method [Brooks and Hughes, 1982], which suppresses convective instabilities in the momentum equation by adding a residual-based upwind perturbation to the test functions in the direction of the relative velocity $\mathbf{c} = \mathbf{v} - \mathbf{w}$. The SUPG stabilization term takes the form

$$\sum_e \int_{\Omega^e(t)} \tau_{\text{SUPG}} \left(\mathbf{c} \cdot \nabla \mathbf{u}\right) \cdot \mathcal{R}_{\text{mom}} \, d\Omega, \tag{54}$$

where $\mathcal{R}_{\text{mom}}$ is the strong-form momentum residual and τ_{SUPG} is an element-level stabilization parameter scaling as $h/(2|\mathbf{c}|)$ in the convection-dominated regime, with h denoting the characteristic element size. The second technique is the *Pressure-Stabilizing/Petrov-Galerkin* (PSPG) method [Hughes et al., 1986], which circumvents the LBB condition by adding a pressure-gradient residual term to the continuity equation, permitting the use of equal-order interpolation functions (e.g., P_1/P_1 or Q_1/Q_1 pairs) while maintaining stability. In the ALE context, both stabilization parameters must be evaluated using the relative velocity $\mathbf{c}$ rather than the absolute material velocity, since it is the relative transport that governs wave propagation and shock-wave thickness on the moving mesh. Furthermore, because the mesh motion $\mathbf{w}$ is an independent variable, the FEM formulation must ensure that the discrete mesh velocity is interpolated using the same basis functions as the geometric mapping. This consistency is vital for maintaining the second-order accuracy of the transport terms and for ensuring that the discrete solution remains compliant with the Geometric Conservation Law (GCL), thereby preventing the emergence of non-physical source terms during significant domain deformation.

Derivation of the ALE Weak Formulation

The weak form is obtained by multiplying the ALE momentum equation by a vector-valued test function $\mathbf{u}$ chosen from the trial space, and integrating over the current physical domain. Because test functions are defined via pull-back from the fixed reference domain $\hat{\Omega}$, they satisfy the fundamental property

$$\left.\frac{\partial \mathbf{u}}{\partial t}\right|_{\hat{\mathbf{x}}} = \mathbf{0}, \tag{55}$$

meaning their referential time derivative vanishes. This substantially simplifies the temporal differentiation of the virtual work and ensures that no spurious terms arise from the movement of the basis function support.

Step 1: Weighting and integration. The strong-form ALE momentum equation,

$$\rho\left(\left.\frac{\partial \mathbf{v}}{\partial t}\right|_{\hat{\mathbf{x}}} + \big[(\mathbf{v}-\mathbf{w})\cdot\nabla\big]\mathbf{v}\right) = \nabla\cdot\boldsymbol{\sigma} + \rho\,\mathbf{f}, \tag{56}$$

where $\boldsymbol{\sigma} = -p\mathbf{I} + 2\mu\,\boldsymbol{\varepsilon}(\mathbf{v})$ is the Cauchy stress tensor and $\boldsymbol{\varepsilon}(\mathbf{v}) = \frac{1}{2}(\nabla\mathbf{v} + \nabla\mathbf{v}^T)$ is the symmetric rate-of-strain tensor, is multiplied by $\mathbf{u}$ and integrated over $\Omega(t)$:

$$\int_{\Omega(t)} \rho\left.\frac{\partial \mathbf{v}}{\partial t}\right|_{\hat{\mathbf{x}}}\cdot\mathbf{u}\,d\Omega + \int_{\Omega(t)} \rho\big[(\mathbf{v}-\mathbf{w})\cdot\nabla\big]\mathbf{v}\cdot\mathbf{u}\,d\Omega = \int_{\Omega(t)} (\nabla\cdot\boldsymbol{\sigma})\cdot\mathbf{u}\,d\Omega + \int_{\Omega(t)} \rho\,\mathbf{f}\cdot\mathbf{u}\,d\Omega. \tag{57}$$

Step 2: Integration by parts of the stress term. Applying the Gauss divergence theorem to the stress integral reduces the smoothness requirements and introduces the natural boundary condition (traction):

$$\int_{\Omega(t)} (\nabla\cdot\boldsymbol{\sigma})\cdot\mathbf{u}\,d\Omega = -\int_{\Omega(t)} \boldsymbol{\sigma} : \nabla\mathbf{u}\,d\Omega + \int_{\partial\Omega(t)} (\boldsymbol{\sigma}\,\mathbf{n})\cdot\mathbf{u}\,d\Gamma, \tag{58}$$

where $\mathbf{n}$ is the outward unit normal on $\partial\Omega(t)$ and $\mathbf{h} = \boldsymbol{\sigma}\,\mathbf{n}$ is the applied traction. The volume integral couples the stress to the gradient of the test function, while the surface integral provides the natural mechanism for imposing FSI traction loads at the interface without any additional algorithmic treatment.

Step 3: Decomposition of the stress bilinear form. Substituting $\boldsymbol{\sigma} = -p\mathbf{I} + 2\mu\,\boldsymbol{\varepsilon}(\mathbf{v})$, the inner volume term splits into a pressure coupling term and a viscous dissipation term:

$$-\int_{\Omega(t)} \boldsymbol{\sigma} : \nabla\mathbf{u}\,d\Omega = \int_{\Omega(t)} p\,(\nabla\cdot\mathbf{u})\,d\Omega - \int_{\Omega(t)} 2\mu\,\boldsymbol{\varepsilon}(\mathbf{v}) : \boldsymbol{\varepsilon}(\mathbf{u})\,d\Omega, \tag{59}$$

where the symmetry of $\boldsymbol{\varepsilon}$ has been used to replace $\boldsymbol{\varepsilon}(\mathbf{v}) : \nabla\mathbf{u}$ with $\boldsymbol{\varepsilon}(\mathbf{v}) : \boldsymbol{\varepsilon}(\mathbf{u})$.

Step 4: Weak continuity constraint. The incompressibility condition $\nabla\cdot\mathbf{v} = 0$ is enforced in a variational sense by multiplying by a scalar test function $q \in L^2(\Omega(t))$ and integrating:

$$\int_{\Omega(t)} q\,(\nabla\cdot\mathbf{v})\,d\Omega = 0. \tag{60}$$

Complete ALE weak system. Assembling all four steps, the full variational problem reads: find $(\mathbf{v}, p) \in \mathcal{V}_t \times \mathcal{Q}_t$ such that for all $(\mathbf{u}, q) \in \mathcal{V}_{t,0} \times \mathcal{Q}_t$,

$$\begin{aligned}
&\int_{\Omega(t)} \rho\left.\frac{\partial \mathbf{v}}{\partial t}\right|_{\hat{\mathbf{x}}}\cdot\mathbf{u}\,d\Omega + \int_{\Omega(t)} \rho\big[(\mathbf{v}-\mathbf{w})\cdot\nabla\mathbf{v}\big]\cdot\mathbf{u}\,d\Omega \\
&\quad + \int_{\Omega(t)} 2\mu\,\boldsymbol{\varepsilon}(\mathbf{v}) : \boldsymbol{\varepsilon}(\mathbf{u})\,d\Omega - \int_{\Omega(t)} p\,(\nabla\cdot\mathbf{u})\,d\Omega = \mathcal{L}(\mathbf{u}), \\
&\int_{\Omega(t)} q\,(\nabla\cdot\mathbf{v})\,d\Omega = 0,
\end{aligned} \tag{61}$$

where $\mathcal{L}(\mathbf{u}) = \int_{\partial\Omega_N(t)} \mathbf{h} \cdot \mathbf{u}\, d\Gamma + \int_{\Omega(t)} \rho \mathbf{f} \cdot \mathbf{u}\, d\Omega$ collects the external traction and body-force contributions. The mesh velocity $\mathbf{w}$ appears exclusively in the convective term; all other operators retain a form identical to a standard Eulerian variational formulation evaluated on the instantaneous configuration $\Omega(t)$.

7.2 Finite Volume Method (FVM)

The Finite Volume Method (FVM) provides a naturally conservative framework for ALE simulations by enforcing the integral balance of a transportable quantity ϕ over a discrete, time-varying control volume $V(t)$. The starting point is the ALE transport identity applied to a single cell. For a scalar field ϕ with source density S_ϕ, integrating over the moving control volume yields the continuous integral conservation law:

$$\frac{d}{dt}\int_{V(t)} \phi\, dV + \oint_{\partial V(t)} \phi\, (\mathbf{v} - \mathbf{w}) \cdot \mathbf{n}\, dA = \int_{V(t)} S_\phi\, dV. \tag{62}$$

Here the surface integral is taken over the moving cell boundary $\partial V(t)$, $\mathbf{n}$ is the outward unit normal, and the relative velocity $(\mathbf{v} - \mathbf{w})$ accounts for the fact that the face itself moves at velocity $\mathbf{w}$.

In practice, the domain is partitioned into a set of non-overlapping cells and the governing equations are integrated over each cell to produce a set of algebraic equations for the cell-averaged values. The cell-averaged value of ϕ is defined as

$$\bar{\phi} = \frac{1}{V(t)} \int_{V(t)} \phi\, dV, \tag{63}$$

so that the total "content" of the cell is $M(t) = V(t)\, \bar{\phi}$. Replacing the continuous surface integral by a summation over the N_f faces of the cell leads to the discrete semi-discrete conservation law in the ALE frame:

$$\frac{d}{dt}(V\bar{\phi}) + \sum_f F_f = SV \tag{64}$$

In this formulation, V denotes the instantaneous volume of the computational cell, and $\bar{\phi}$ represents the volume-averaged value of the scalar field. The first term, $\frac{d}{dt}(V\bar{\phi})$, encapsulates the total rate of change of the integrated quantity within the deforming cell. By applying the product rule, this term can be decomposed into a part representing the intrinsic change of the field and a part representing the volumetric expansion or contraction of the cell. This dual dependency is what allows the ALE-FVM to maintain conservation as the mesh deforms to follow boundaries or resolve flow features.

The second term, $\sum_f F_f$, represents the net numerical flux across the faces f of the control volume. In the ALE context, these fluxes are fundamentally different from their Eulerian counterparts because they must account for the relative velocity between the fluid and the moving mesh faces. The source term SV accounts for any internal generation or consumption of the quantity within the cell volume.

A significant challenge in the ALE-FVM implementation is the requirement for temporal consistency between the volume update and the flux evaluation. Since the cell volume V is a function of time, the discrete approximation of the time derivative $\frac{d}{dt}(V\bar{\phi})$ must be precisely synchronized with the geometric change of the cell. If the numerical scheme for the time derivative is not algorithmically matched to the swept volume calculated by the face fluxes, the solver will introduce "geometric residuals" (non-physical source terms that violate the DGCL). Consequently, the robustness of an ALE-FVM solver is often limited by the choice of time-stepping scheme; for instance, using a second-order backward differentiation formula (BDF2) requires a similarly high-order approximation for the mesh velocity and the face areas to prevent the accumulation of geometric errors.

7.3 ALE Flux

In the Finite Volume discretization of the ALE equations, the numerical flux F_f across a face f represents the net rate of advective transport of the scalar field ϕ. Unlike standard Eulerian formulations, where the flux depends solely on the material velocity $\mathbf{v}$, the ALE framework requires the evaluation of transport relative to the motion of the grid. The face flux can be decomposed into two physically distinct contributions:

$$F_f = \underbrace{\int_{A_f} \phi\,(\mathbf{v}\cdot\mathbf{n})\,dA}_{\text{Advective flux (material)}} - \underbrace{\int_{A_f} \phi\,(\mathbf{w}\cdot\mathbf{n})\,dA}_{\text{Geometric flux (mesh sweeping)}} . \tag{65}$$

The first term is the standard Eulerian advective flux driven by the material velocity; the second term is the "geometric flux" which accounts for the volume swept by the moving face. Together, only their difference (the transport relative to the mesh) contributes to the net change of ϕ inside the cell.

At the discrete level this is approximated by evaluating the integrands at the face center, giving:

$$F_f \approx \phi_f(\mathbf{v}_f - \mathbf{w}_f)\cdot\mathbf{n}_f A_f \tag{66}$$

In this expression, $(\mathbf{v}_f - \mathbf{w}_f)$ defines the relative (or convective) velocity at the face, $\mathbf{n}_f$ is the unit normal vector, and A_f is the face area. As illustrated in Figure 7, the amount of property ϕ passing through a control volume boundary is determined by the component of the fluid velocity that exceeds the mesh velocity in the direction of the face normal.

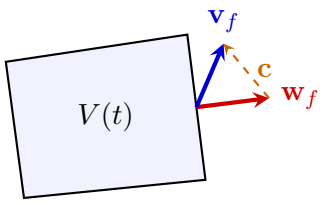

Figure 7: Visualization of the relative convective flux on a moving cell face. The mesh velocity $\mathbf{w}$ modulates the effective transport; even in a static fluid ($\mathbf{v} = 0$), a moving face creates a numerical flux proportional to $(-\mathbf{w}\cdot\mathbf{n})$.

Physically, this relative flux provides the mechanism by which the ALE method transitions between different kinematic descriptions. If the mesh velocity $\mathbf{w}_f$ is set equal to the normal component of the fluid velocity $\mathbf{v}_f\cdot\mathbf{n}_f$, the advective flux F_f vanishes locally, effectively treating the face as a material surface. Conversely, when the mesh is stationary ($\mathbf{w}_f = \mathbf{0}$), the expression recovers the classical Eulerian flux. This flexibility allows the mesh to "absorb" a portion of the convective transport, which is particularly advantageous for minimizing numerical diffusion in regions of high-speed flow where a purely Eulerian grid would require extreme refinement.

However, the accuracy of the ALE flux is highly sensitive to the reconstruction of the face-centered values ϕ_f and $\mathbf{v}_f$ from the cell-centered data. Standard interpolation schemes, such as upwind or central differencing, must be applied to the relative velocity field rather than the absolute velocity to ensure stability. Because the face area A_f and the normal $\mathbf{n}_f$ are time-dependent, they must be evaluated at the correct temporal location within the time step, typically at the midpoint or at the end of the interval, to maintain second-order accuracy. Inconsistencies in these geometric evaluations can lead to a violation of the Discrete Geometric Conservation Law (DGCL), manifesting as spurious oscillations in the conserved field ϕ even in the presence of uniform flow.

In the ALE context, numerical stability for convection-dominated flows is maintained through upwinding with respect to the *relative* velocity field $\mathbf{c} = \mathbf{v} - \mathbf{w}$. The donor-cell (first-order up-

wind) reconstruction selects the face value ϕ_f from whichever neighbouring cell lies upstream of the relative flow:

$$\phi_f = \begin{cases} \phi_L & \text{if } (\mathbf{v}_f - \mathbf{w}_f) \cdot \mathbf{n}_f > 0, \\ \phi_R & \text{if } (\mathbf{v}_f - \mathbf{w}_f) \cdot \mathbf{n}_f < 0, \end{cases} \tag{67}$$

where ϕ_L and ϕ_R are the values in the left and right cells sharing face f. The sign of the relative normal flux $(\mathbf{v}_f - \mathbf{w}_f) \cdot \mathbf{n}_f$ determines the direction of information propagation. This criterion correctly accounts for the mesh motion: if the mesh moves faster than the fluid in the direction of $\mathbf{n}_f$, the relative velocity changes sign and the donor cell switches sides, ensuring that information is never extrapolated against the physical transport direction. A complementary requirement enforced alongside the upwinding is the discrete volume update consistency condition:

$$V^{n+1} = V^n + \Delta t \sum_f (\mathbf{w}_f \cdot \mathbf{n}_f \, A_f), \tag{68}$$

which guarantees that the cell volume change over the time step is exactly equal to the volume swept by all bounding faces moving at velocity $\mathbf{w}_f$. Satisfying this equation in concert with the flux evaluation is precisely the statement of the Discrete Geometric Conservation Law (DGCL); any inconsistency between the volume update and the face-swept volume introduces an algebraic residual that manifests as a spurious mass source, independent of the mesh quality or the time-step size.

7.4 Time Integration

The temporal discretization of the ALE-governed transport equations necessitates a rigorous treatment of the product rule, as both the scalar field ϕ and the control volume V are time-dependent variables. In a discrete sense, the total rate of change of the integrated quantity within a moving cell must be decomposed into its constituent physical and geometric parts. Applying the Leibniz rule for the differentiation of an integral over a moving domain leads to the following expansion:

$$\frac{d}{dt}(V\phi) = V\frac{\partial \phi}{\partial t} + \phi \frac{\partial V}{\partial t}. \tag{69}$$

This decomposition highlights a fundamental challenge in ALE time-stepping: the numerical update of the field ϕ is intrinsically coupled to the rate of change of the cell volume. The first term on the right-hand side, $V\frac{\partial \phi}{\partial t}$, represents the local rate of change of the property as perceived in the referential frame. The second term, $\phi\frac{\partial V}{\partial t}$, acts as a "geometric source" that accounts for the dilution or concentration of the field caused by the expansion or contraction of the mesh.

For a numerical scheme to be considered robust, the discretization of $\frac{\partial V}{\partial t}$ must be algorithmically consistent with the swept volume calculated by the ALE fluxes across the cell faces. If this consistency is not maintained (for instance, if the volume change is calculated using an end-of-step configuration V^{n+1} while the fluxes are evaluated at a midpoint $\Delta t/2$), the solver will introduce a first-order temporal error that manifests as a violation of the DGCL.

In practice, higher-order time-integration methods such as the second-order Backward Differentiation Formula (BDF2) or the Crank-Nicolson scheme require the evaluation of the cell volume and the mesh velocity at multiple sub-steps. This ensures that the geometric variation of the domain is resolved with the same order of accuracy as the fluid transport. A primary limitation of this coupling is the increased computational cost, as the system matrices (in FEM) or the flux reconstructors (in FVM) must be recomputed at every time level to reflect the updated mesh metric. However, this cost is a necessary prerequisite for preventing the accumulation of non-physical "geometric residuals" which, if left unaddressed, would lead to the loss of global conservation in long-term transient simulations.

To make these ideas concrete, consider the two most common one-step schemes applied to the semi-discrete ALE cell equation $\frac{d}{dt}(V\bar{\phi}) + \sum_f F_f = 0$. The explicit (forward) Euler scheme evaluates all fluxes and mesh velocities at the known time level t^n:

$$V^{n+1}\phi^{n+1} = V^n\phi^n - \Delta t \sum_f F_f(\phi^n, \mathbf{w}^n). \tag{70}$$

While simple to implement, this scheme is conditionally stable and subject to a Courant-type restriction on Δt based on the *relative* velocity $|\mathbf{c}| = |\mathbf{v} - \mathbf{w}|$. The implicit (backward) Euler scheme instead evaluates the fluxes at the updated time level t^{n+1}:

$$V^{n+1}\phi^{n+1} = V^n\phi^n - \Delta t \sum_f F_f(\phi^{n+1}, \mathbf{w}^{n+1}). \tag{71}$$

This scheme is unconditionally stable and is the basis for most production ALE solvers. Both schemes must compute V^{n+1} using the DGCL-consistent volume update (see the preceding section) rather than from the updated node coordinates independently; failure to do so couples a first-order geometric error into an otherwise higher-order temporal discretization. A common practical approach in partitioned FSI codes is a "staggered" sequence: first advance the mesh ($\mathbf{w}^{n+1}$ and V^{n+1} via the DGCL), then solve the implicit fluid system on the updated geometry. This ordering is computationally efficient but may introduce an "added-mass" instability when the fluid-to-solid density ratio is large; iterative sub-cycling or a monolithic solver may then be required to restore stability.

8 Mesh Motion Strategies

The practical utility of the ALE framework depends fundamentally on the ability to prescribe a mesh velocity field $\mathbf{w}$ that maintains the geometric quality of the computational grid throughout the simulation. While the ALE formulation theoretically permits any arbitrary mesh motion, numerical stability and spatial accuracy require that the mapping from the referential domain $\hat{\Omega}$ to the physical domain $\Omega(t)$ remains a valid diffeomorphism. Beyond mere geometry, the choice of $\mathbf{w}$ directly influences the transport physics of the system; as established in previous sections, the mesh velocity dictates the relative convective flux across the cell faces. A poorly behaved mesh motion field can introduce significant numerical artifacts, excessive diffusion, or even lead to immediate solver failure if the mapping becomes non-bijective.

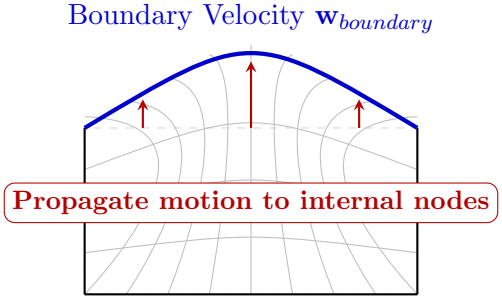

Figure 8: The Mesh Motion Problem: Boundary displacements, typically derived from FSI or free-surface physics, must be propagated to internal nodes to maintain element health and prevent negative volumes.

In practice, the mesh must be updated to accommodate moving boundaries (such as those found in fluid-structure interaction or free-surface problems) while minimizing element distortion, skewness, and the risk of cell inversion. Mesh motion strategies act as the algorithmic tools

used to propagate these boundary displacements into the interior of the domain. These strategies range from computationally efficient smoothing operators to more robust, physics-based analogies that treat the mesh as a deformable continuum. By defining the mesh as a fictitious elastic solid or a diffusive medium, the solver can automatically redistribute grid nodes in a way that preserves the integrity of the spatial discretization even under significant boundary excursions.

The selection of a specific strategy involves a critical trade-off between the computational cost of the mesh update and the ability of the grid to withstand deformation before spatial discretization errors become prohibitive. While simple Laplacian smoothing is fast, it often fails to preserve boundary layer resolution in high-gradient regions. Conversely, the elastic analogy is more robust but requires the solution of an additional system of equations at every time step. This section explores the hierarchy of these techniques, detailing how different formulations, from simple differential smoothing to the eventual necessity of global remeshing, manage the evolution of the spatial domain $\Omega(t)$.

Before examining the individual strategies, it is useful to define the quantitative criteria used to assess whether the current mesh remains numerically admissible or whether intervention is necessary. Table 3 summarizes the most commonly employed mesh quality metrics in ALE solvers.

Table 3: Common mesh quality metrics used in ALE solvers to detect element degradation and trigger mesh smoothing or remeshing.

Metric	**Definition**	**Ideal value**	**Critical threshold**
Jacobian J	$\det(\partial \mathbf{x}/\partial \hat{\mathbf{x}})$	$J > 0$	$J \leq 0$ (inversion)
Minimum J ratio	$J_{\min}/J_{\max}$ within element	1.0	< 0.2
Aspect ratio	$h_{\max}/h_{\min}$	1.0	$> 10^3$
Skewness	$1 - (\hat{\theta}/\theta_{\text{opt}})$, normalized angle deviation	0.0	> 0.85
Orthogonality	$\min_f \lvert\cos \angle(\mathbf{n}_f, \mathbf{d}_{LR})\rvert$	1.0	< 0.05
Condition number	$\kappa(\mathbf{F}) = \lVert\mathbf{F}\rVert\lVert\mathbf{F}^{-1}\rVert$	1.0	$> 10^6$

Among these, the Jacobian determinant J is the most fundamental: a negative value signals that the ALE mapping $\boldsymbol{\chi}$ has ceased to be a diffeomorphism, rendering all subsequent computations on that element meaningless. The remaining metrics provide early-warning indicators that allow the solver to initiate mesh smoothing before the geometry reaches a critical state.

8.1 Laplacian Smoothing

The most computationally efficient method for determining the mesh velocity field $\mathbf{w}$ is Laplacian smoothing, which treats the distribution of boundary displacements as a steady-state diffusion process. A historically important and closely related approach is the spring analogy introduced by Batina [1990], in which each mesh edge connecting nodes i and j is replaced by a fictitious spring of stiffness K_{ij}. The static equilibrium of node i then requires that the net spring force vanishes:

$$\sum_{j \in \mathcal{N}(i)} K_{ij} \left(\mathbf{x}_j^{\text{new}} - \mathbf{x}_i^{\text{new}} \right) = \mathbf{0}, \tag{72}$$

where $\mathcal{N}(i)$ denotes the set of nodes directly connected to i by an edge. With uniform stiffness $K_{ij} = 1$ for all edges, this system reduces identically to the discrete five-point (or seven-point in 3D) Laplacian stencil, establishing the mathematical equivalence of the spring analogy and Laplacian smoothing for regular meshes. Figure 9 illustrates the equilibrium of an interior node i with its four mesh-edge springs. In the continuum limit, the mesh velocity is governed by

the Laplace equation, effectively serving as a harmonic extension of the Dirichlet boundary conditions prescribed at the moving interfaces:

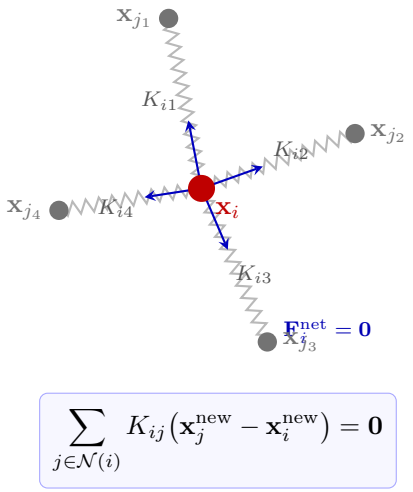

Figure 9: Spring analogy for mesh motion [Batina, 1990]. Each mesh edge connecting an interior node i (red) to a neighbour j_k (black) is replaced by a fictitious spring of stiffness K_{ij}. The updated position of i is found by requiring the net spring force (blue arrows) to vanish. With uniform stiffness $K_{ij} = 1$, the equilibrium equation reduces to the discrete Laplacian stencil $\mathbf{x}_i = |\mathcal{N}(i)|^{-1} \sum_j \mathbf{x}_j$, showing the mathematical equivalence of the spring analogy and Laplacian smoothing.

$$\nabla^2 \mathbf{w} = 0 \quad \text{on } \Omega, \qquad \mathbf{w} = \mathbf{w}_{\text{boundary}} \quad \text{on } \partial\Omega. \tag{73}$$

The use of an elliptic operator ensures that the mesh velocity field is infinitely differentiable within the interior of the domain, provided the boundary motion is continuous. Physically, this formulation implies that the velocity of an internal mesh node is the weighted average of the velocities of its neighbors. This averaging property is highly effective at preventing local "kinks" or non-physical oscillations in the grid, as it naturally tends to maintain a uniform spacing between nodes in regions where the initial mesh was equidistant.

However, the primary limitation of Laplacian smoothing lies in its uniform treatment of the spatial domain. Because the operator assumes a constant diffusion coefficient, it lacks the ability to distinguish between large elements in the far-field and highly refined elements near a boundary. In simulations involving boundary layers or complex geometries, the small, high-aspect-ratio elements are often the first to undergo significant distortion. Since the Laplacian operator distributes the total deformation evenly across the domain, these smaller cells may become compressed or inverted long before the larger cells have absorbed their share of the displacement. Consequently, while Laplacian smoothing is suitable for problems with moderate deformation and relatively uniform meshes, it often fails in high-fidelity fluid-structure interaction (FSI) scenarios where preserving the integrity of a refined near-wall mesh is critical.

8.2 Variable Diffusion

To overcome the tendency of Laplacian smoothing to disproportionately distort small elements, the mesh motion equation is modified by introducing a spatially varying diffusion coefficient γ. This formulation, known as variable diffusion mesh smoothing, governs the distribution of the mesh velocity $\mathbf{w}$ through the following elliptic partial differential equation:

$$\nabla \cdot (\gamma \nabla \mathbf{w}) = 0. \tag{74}$$

In this context, the coefficient γ acts as a local "stiffness" parameter for the mesh. By assigning higher values of γ to regions containing smaller or more critical elements, such as those within a fluid boundary layer, the mesh in these zones becomes more resistant to deformation. Consequently, the boundary displacements are preferentially absorbed by the larger, less sensitive elements in the far-field, where γ is relatively small.

The efficacy of this strategy depends entirely on the definition of the diffusion field $\gamma(\mathbf{x}, t)$. Common implementations define γ as a function of the geometric properties of the mesh, such as the inverse of the cell volume $(1/V)$ or the inverse of the distance from the nearest moving boundary $(1/d^n)$. By making the mesh "stiffer" near the interfaces, the orthogonality and aspect ratio of near-wall elements are preserved for much larger boundary displacements than would be possible with uniform smoothing. This localized protection is essential for maintaining the accuracy of wall-shear stress calculations and preventing the non-physical pressure oscillations that arise from poorly shaped elements.

However, the introduction of variable diffusion increases the complexity of the ALE framework. Unlike the linear Laplacian operator, a diffusion coefficient that depends on the instantaneous cell volume $V(t)$ renders the mesh motion equation non-linear, requiring iterative solvers or lagging techniques within each time step. Furthermore, the selection of the exponent n in distance-based functions requires empirical tuning; if γ varies too abruptly, it may lead to poor conditioning of the linear system or create artificial "shear layers" within the mesh itself where the stiffness gradient is high. Despite these challenges, variable diffusion remains a standard industry practice for complex fluid-structure interaction (FSI) problems where mesh topology preservation is paramount.

8.3 Elastic Analogy

For simulations involving complex boundary deformations or rotational motions, the mesh is often treated as a pseudo-structural continuum governed by the equations of linear elasticity [Johnson and Tezduyar, 1994]. In this framework, the mesh velocity $\mathbf{w}$ (or the incremental mesh displacement) is determined by solving the equilibrium equation for a fictitious stress field $\boldsymbol{\sigma}_{mesh}$:

$$\nabla \cdot \boldsymbol{\sigma}_{mesh} = 0. \tag{75}$$

By invoking the linear elastic constitutive law $\boldsymbol{\sigma}_{mesh} = \lambda_m(\nabla \cdot \mathbf{d})\mathbf{I} + \mu_m(\nabla \mathbf{d} + \nabla \mathbf{d}^T)$, where $\mathbf{d}$ is the incremental mesh displacement and λ_m, μ_m are the fictitious Lamé parameters of the mesh material, substitution into the equilibrium equation yields the Navier-Cauchy system:

$$\mu_m \Delta \mathbf{d} + (\lambda_m + \mu_m)\, \nabla(\nabla \cdot \mathbf{d}) = \mathbf{0}. \tag{76}$$

This coupled elliptic system governs the distribution of mesh displacements throughout the domain, subject to Dirichlet conditions $\mathbf{d} = \mathbf{d}_{\text{boundary}}$ at moving interfaces and $\mathbf{d} = \mathbf{0}$ at fixed walls. The ratio $\nu_m = \lambda_m/(2(\lambda_m + \mu_m))$, interpreted as a fictitious Poisson's ratio, controls the degree of coupling between the coordinate components; setting $\nu_m \to 0$ recovers the scalar Laplacian limit, while $\nu_m \to 0.5$ approaches the nearly incompressible regime, which tends to preserve element volumes. Unlike the scalar Laplacian smoothing, which treats each component of the mesh velocity independently, the elastic analogy couples the displacement components through the Poisson effect.

The primary kinematic advantage of the elastic analogy is its superior preservation of element shape and angular integrity. Because the formulation accounts for shear stresses within the "mesh material," the elements resist skewing and shearing more effectively than they would under pure diffusion. This property is particularly beneficial in regions of high vorticity or near rotating boundaries, where Laplacian-based methods often lead to severe mesh entanglement. Furthermore, the "stiffness" of the mesh can be spatially modulated by varying the Young's modulus as a function of the cell volume or the distance from the boundary, similar to the

variable diffusion approach. By increasing the modulus in refined regions, the small elements are rendered nearly rigid, forcing the larger far-field elements to accommodate the bulk of the deformation.

Despite its robustness, the elastic analogy entails a significantly higher computational overhead. While Laplacian smoothing requires the solution of d uncoupled scalar equations (where d is the number of spatial dimensions), the elastic analogy requires solving a coupled system of d equations. This increases the memory footprint and the CPU time required for the mesh update step. Additionally, for very large deformations, a linear elastic model may eventually fail as the small-strain assumption is violated; in such cases, non-linear hyperelastic models may be employed to prevent element inversion, albeit at the cost of solving a non-linear system of equations at each time step.

8.4 Remeshing

While smoothing and elastic analogies effectively manage moderate mesh deformations, they are fundamentally constrained by the fixed topological connectivity of the initial grid. In simulations involving extreme boundary displacements (such as large-scale fluid-structure interactions, crack propagation, or high-vorticity flows), the mesh elements may eventually reach a state of geometric degradation where the Jacobian J approaches zero or becomes negative. At this critical threshold, the mapping between the referential and spatial domains is no longer a diffeomorphism, and the simulation will inevitably diverge. To circumvent this, a remeshing procedure is triggered, wherein the existing, distorted mesh is replaced by a high-quality grid with a new topological structure.

The initiation of remeshing is governed by a set of objective mesh quality metrics, typically including the cell aspect ratio, the maximum skewness, and the condition number of the element transformation matrix. Once these metrics exceed a predefined tolerance, the current state of the simulation is paused, and a new discretization of the instantaneous spatial domain $\Omega(t)$ is generated. This process is inherently discrete and necessitates a data transfer step, often referred to as a projection or remapping. During this phase, the field variables (e.g., velocity, pressure, and density) are interpolated from the old, distorted grid to the new, optimized grid.

The primary limitation of remeshing is the introduction of numerical diffusion and projection errors. Each remapping event involves a degree of smoothing as the solution is interpolated across disparate connectivity patterns, which can lead to the loss of high-frequency details or the violation of local conservation laws if not handled with a strictly conservative projection algorithm. Furthermore, the remeshing process breaks the temporal smoothness of the mesh velocity field $\mathbf{w}$, necessitating a restart of the time-integration scheme or a careful initialization of the mesh velocities on the new grid to satisfy the Discrete Geometric Conservation Law (DGCL). Despite these drawbacks, remeshing remains a vital "last resort" that extends the applicability of the ALE framework to the most challenging regimes of continuum mechanics, where the Lagrangian-like tracking of boundaries would otherwise lead to total grid failure.

9 Fluid–Structure Interaction (FSI)

The simulation of Fluid–Structure Interaction (FSI) requires the simultaneous solution of the equations governing fluid dynamics and structural mechanics, linked by a set of consistency conditions at the common interface $\Gamma(t)$ [Donea et al., 1982, 2004]. The ALE framework is particularly advantageous in this context, as it allows the fluid mesh to be treated as a deformable medium that conforms to the structural motion. This ensures that the interface is resolved explicitly as a boundary of the fluid domain, rather than being captured through diffuse-interface or immersed methods. Successful FSI coupling depends on maintaining both kinematic continuity (velocity matching) and dynamic equilibrium (traction balancing) across the interface,

while ensuring that the mesh motion is strictly synchronized with the structural displacement.

9.1 Interface Conditions

The physical coupling between the fluid and solid subdomains is governed by two fundamental transmission conditions enforced at the common interface $\Gamma(t)$. These conditions ensure that the two distinct physical continua behave as a single, synchronized system. In the ALE framework, where the interface is explicitly tracked by the moving mesh, these conditions are categorized into kinematic continuity and dynamic equilibrium, as illustrated in Figure 10.

The first condition is **kinematic continuity**, which ensures that the fluid and solid do not "detach" or "overlap" during the simulation. This requires the fluid velocity $\mathbf{v}_f$ and the structural velocity $\mathbf{v}_s$ to be identical at every point on the interface:

$$\mathbf{v}_f = \mathbf{v}_s \quad \text{on } \Gamma(t). \tag{77}$$

For viscous flows, this identity represents the no-slip condition on a moving wall. Physically, it dictates that the fluid particles adjacent to the solid must move synchronously with the boundary, preventing the non-physical formation of vacuums or the penetration of one domain into the other. In a discrete ALE setting, this condition is particularly convenient because the mesh velocity at the interface $\mathbf{w}$ is typically set equal to $\mathbf{v}_s$, which effectively reduces the relative convective flux across the boundary to zero.

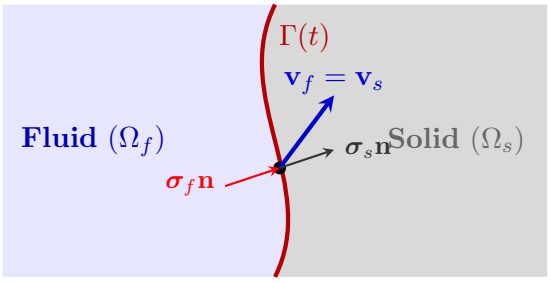

Figure 10: Visualization of the FSI interface $\Gamma(t)$. The kinematic condition ensures velocity continuity, while the dynamic condition ensures that fluid traction is perfectly balanced by the structural load.

The second condition is **dynamic equilibrium**, or traction balance, which stems from Newton's Third Law of motion. It ensures that the fluid traction matches the structural load, requiring that the forces exerted by the fluid on the solid be equal and opposite to the forces exerted by the solid on the fluid:

$$\boldsymbol{\sigma}_f\mathbf{n} = \boldsymbol{\sigma}_s\mathbf{n} \quad \text{on } \Gamma(t). \tag{78}$$

In this expression, $\boldsymbol{\sigma}_f$ and $\boldsymbol{\sigma}_s$ denote the fluid and solid Cauchy stress tensors, respectively, and $\mathbf{n}$ is the unit normal vector at the interface. The fluid stress includes both hydrostatic pressure and viscous shear components. This condition is essential for the exchange of energy between fields; the fluid forces deform the structure, while the resulting structural deformation modifies the flow topology.

Mathematically, the simultaneous satisfaction of these conditions is the primary source of complexity in FSI problems. In a numerical implementation, the kinematic condition is typically treated as a Dirichlet boundary condition for the fluid subproblem, while the dynamic condition acts as a Neumann load for the structural subproblem. The stability of the overall ALE simulation depends heavily on the temporal accuracy with which these two conditions are synchronized, especially in cases involving strong added-mass effects where fluid and solid densities are of a similar order of magnitude [Causin et al., 2005].

9.2 Mesh Boundary Condition

In the ALE framework, the mesh velocity $\mathbf{w}$ is an independent kinematic variable within the interior of the domain, but it is strictly constrained at the boundaries to satisfy the geometric requirements of the physical system. In the specific context of Fluid–Structure Interaction (FSI), the mesh must track the motion of the deformable solid to maintain a continuous and conforming interface. This requirement is enforced by prescribing a Dirichlet boundary condition for the mesh velocity field at the fluid–structure interface $\Gamma(t)$:

$$\mathbf{w} = \mathbf{v}_s \quad \text{on } \Gamma(t). \tag{79}$$

This identity ensures that the mesh nodes located on the interface move synchronously with the structural velocity $\mathbf{v}_s$. By imposing this condition, the interface is treated in a purely Lagrangian manner, which prevents the formation of non-physical gaps or overlaps between the fluid and solid subdomains.

The primary kinematic consequence of this boundary condition is the simplification of the advective transport terms at the interface. Since $\mathbf{w} = \mathbf{v}_s$ and the fluid velocity $\mathbf{v}_f$ must also equal $\mathbf{v}_s$ due to the no-slip condition, the relative velocity $\mathbf{c} = \mathbf{v}_f - \mathbf{w}$ vanishes identically at the boundary. This eliminates the convective flux across the interface, ensuring that mass and momentum are transported solely through the physical motion of the boundary rather than through numerical flux reconstruction.

However, the prescription of $\mathbf{w}$ on $\Gamma(t)$ only defines the mesh motion at the boundary; the velocity of the interior nodes must still be determined using the smoothing or elastic strategies previously detailed. The boundary condition acts as the "driver" for the interior mesh deformation. A critical limitation of this approach arises during large structural rotations or extreme topological changes; while the interface condition ensures a perfect match at the boundary, the resulting displacement field may lead to severe element distortion or inversion in the interior of the fluid domain. In such cases, the ALE mapping loses its bijective property, and the boundary condition must be supplemented with localized remeshing or mesh regularization to preserve the stability of the simulation.

9.3 Coupling Strategies

The simultaneous solution of the fluid and structural equations, linked by the nonlinear interface conditions, necessitates a robust coupling strategy. Within the ALE framework, the choice of coupling determines the temporal synchronization of the fluid velocity, the structural displacement, and the mesh velocity. These strategies are broadly categorized into partitioned and monolithic approaches, reflecting the degree of integration between the subproblem solvers.

The partitioned (or staggered) approach treats the fluid and solid as separate computational entities, utilizing distinct solvers for each physics domain. In a typical iteration, the fluid subproblem is solved first to determine the interface tractions, which are then passed as a load to the structural solver. The resulting structural displacement is used to update the mesh geometry and the mesh velocity $\mathbf{w}$, providing a new boundary condition for the next fluid time step.

- **Advantages and Limitations:** The primary benefit of partitioned schemes is the ability to reuse highly optimized, standalone codes for both the fluid and the structure. However, this decoupling often leads to a lag in the interface conditions, which can trigger numerical instabilities. This is particularly prevalent in cases with a high fluid-to-structure density ratio, known as the artificial added-mass effect [Causin et al., 2005], where the fluid's inertia significantly influences the structural response. To maintain stability, partitioned schemes often require sub-iterations within each time step (strongly coupled partitioned) or extremely small time increments, significantly increasing the total computational time.

In contrast, the monolithic approach formulates the fluid, structure, and mesh equations into a single, unified system of algebraic equations. The entire system is solved simultaneously at each time step, typically using a Newton-Raphson or similar iterative method. This ensures that the kinematic and dynamic interface conditions are satisfied exactly at the end of every iteration, providing superior stability and temporal consistency compared to partitioned methods.

- **Complexity and Performance:** While monolithic schemes are inherently stable and immune to the added-mass effect, they entail a significantly higher level of implementation complexity. The resulting global system matrix is often ill-conditioned due to the disparate physical scales and different types of partial differential equations being coupled. The construction of the cross-term Jacobians, which represent the sensitivity of the fluid residual to structural displacement, is also mathematically demanding and memory-intensive. Consequently, monolithic solvers are often reserved for cases where strong coupling is physically unavoidable, such as the simulation of blood flow in highly compliant arteries or the aeroelasticity of lightweight membranes.

The selection of a coupling strategy is therefore a balance between the modularity of the software architecture and the physical requirements of the interaction. For most engineering applications with high structural stiffness, partitioned methods are preferred for their flexibility; however, as the mass ratio approaches unity or the structure becomes increasingly compliant, the monolithic approach becomes the only viable path to a stable and accurate solution.

To make the partitioned algorithm concrete, the typical loosely coupled (one-pass stagger) procedure for a single time step $[t^n, t^{n+1}]$ is summarized in Table 4.

Table 4: Loosely coupled (staggered) partitioned ALE-FSI algorithm for one time step $[t^n, t^{n+1}]$.

Step	**Operation**	**Domain / quantity updated**
1	Predict structural displacement: $\mathbf{d}_s^{n+1,0} \leftarrow$ extrapolation	Solid Ω_s
2	Prescribe interface BC: $\mathbf{w}\|_\Gamma \leftarrow \mathbf{v}_s^{n+1,0}$	Interface $\Gamma(t)$
3	Solve mesh motion equation ($\nabla^2 \mathbf{w} = 0$ or Navier-Cauchy)	Fluid mesh $\hat{\Omega}$
4	Update node positions: $\mathbf{x}^{n+1} \leftarrow \mathbf{x}^n + \Delta t\, \mathbf{w}^{n+1}$ (DGCL)	Fluid mesh $\Omega_f(t)$
5	Solve ALE fluid equations for $(\mathbf{v}_f^{n+1}, p^{n+1})$	Fluid Ω_f
6	Compute interface traction: $\mathbf{h} \leftarrow \boldsymbol{\sigma}_f \mathbf{n}\|_\Gamma$	Interface $\Gamma(t)$
7	Solve structural equations with traction load $\mathbf{h}$	Solid Ω_s
8	Check convergence; if strongly coupled, repeat from Step 2	—

The added-mass instability arises primarily in Step 5–7 when the fluid and structural inertias are of similar magnitude: the one-pass stagger introduces a half-step phase lag in the interface traction, which acts as a negative damping force on the structure. In that regime, the iteration from Steps 2–7 must be sub-cycled to convergence within each time step, transforming the loosely coupled scheme into a strongly coupled partitioned (SCP) algorithm with substantially increased cost but recovered stability.

10 Limitations and Alternatives

The Arbitrary Lagrangian-Eulerian framework represents a sophisticated compromise between the spatial and material descriptions of continuum mechanics. By allowing the computational grid to move independently of the fluid velocity, ALE effectively resolves boundary layers and tracks material interfaces with second-order accuracy. However, the method is not a universal

solution for all moving boundary problems. Its fundamental reliance on a conforming mesh mapping (a diffeomorphism between the referential and spatial configurations) imposes strict requirements on the smoothness and magnitude of the mesh deformation. When these requirements are violated, the mathematical and computational integrity of the ALE description is compromised. This section examines the conditions under which ALE becomes suboptimal and explores alternative methodologies designed to handle extreme topological changes.

10.1 Limitations of ALE

The Arbitrary Lagrangian-Eulerian (ALE) method, while offering high-fidelity interface tracking, is fundamentally constrained by the requirement that the mapping between the referential domain and the physical domain remains a diffeomorphism. This mathematical requirement ensures that the Jacobian J remains positive and that the mesh connectivity remains valid. However, in complex fluid dynamics and high-strain structural interactions, several critical limitations emerge.

The primary technical hurdle is **mesh distortion**. As the physical domain $\Omega(t)$ undergoes non-uniform deformation (such as high-shear flow or localized structural buckling), the mesh velocity field $\mathbf{w}$ may fail to maintain element regularity. When elements become highly skewed or aspect ratios become extreme, the numerical accuracy of the spatial gradients (e.g., $\nabla\phi$ or $\Delta\mathbf{v}$) degrades significantly. In the limit, an element may "invert," resulting in a non-physical negative Jacobian ($J \leq 0$). This singular state leads to the immediate divergence of the numerical solver, as the transformation between coordinates is no longer bijective. Even before inversion occurs, severe distortion increases the condition number of the system matrices, slowing linear solver convergence and introducing significant truncation errors.

The standard ALE framework is also incapable of handling **topological changes** in the domain. Because the method relies on a fixed connectivity mapping, it cannot naturally represent processes such as the breakup of a fluid droplet, the merging of two free surfaces, or the fragmentation of a solid structure. In these scenarios, the interface $\Gamma(t)$ undergoes a fundamental change in its manifold structure. A body-conforming ALE mesh, which is "tethered" to the interface, cannot adapt to these changes without a discontinuous jump in its connectivity. Consequently, ALE is typically restricted to problems where the topology of the subdomains remains invariant throughout the simulation.

Finally, the reliance on **remeshing** to mitigate distortion introduces a substantial computational and numerical overhead. When the mesh quality drops below a critical threshold, the simulation must be paused to generate a new mesh and project the solution variables from the old grid to the new one. This remapping process is computationally expensive (involving search algorithms and high-order interpolations) and also introduces numerical diffusion. This "projection error" can lead to the loss of conservation for mass or momentum if the interpolation is not strictly conservative. For transient problems requiring frequent remeshing, the cumulative diffusion can significantly dampen physical oscillations or dissipate fine-scale turbulent structures, undermining the very precision that the ALE method is intended to provide.

10.2 Alternative Methodologies

When the physical requirements of a simulation exceed the topological constraints of the ALE framework, such as during the coalescence of droplets, the fragmentation of solids, or extreme splashing, practitioners typically transition from interface-tracking to interface-capturing or non-conforming mesh methods. These alternatives decouple the description of the interface from the motion of the underlying computational grid, typically utilizing a fixed Eulerian background mesh to circumvent the issues of mesh distortion and inversion.

The most prominent interface-capturing paradigms are the Volume of Fluid (VOF) and Level-set methods, which represent the interface implicitly through the transport of an auxiliary

scalar field. In the VOF approach [Hirt and Nichols, 1981], the interface is tracked by evolving a volume fraction field C, representing the portion of a cell occupied by a specific phase. The primary advantage of VOF is its inherent adherence to global mass conservation, as the integral of the volume fraction is preserved by the discrete transport operator. However, because C is a discontinuous step function, the interface must be reconstructed at each time step, typically using Piecewise Linear Interface Calculation (PLIC), to compute surface tension and curvature.

In contrast, Level-set methods [Osher and Sethian, 1988] provide a mathematically smooth alternative by representing the interface as the zero-contour of a continuous signed distance function ϕ. This formulation allows for the analytic calculation of geometric properties, such as unit normals and curvature, which are critical for surface-tension-dominated flows. However, unlike ALE or VOF, Level-set methods are not naturally conservative; numerical errors in the transport of ϕ can lead to a non-physical loss or gain of mass.

A further departure from the body-conforming ALE approach is found in the Immersed Boundary Method (IBM) [Peskin, 2002], which is categorized as a non-conforming or fixed-grid coupling strategy. In IBM, the fluid equations are solved on a stationary Eulerian grid, while the solid structure is represented by an independent Lagrangian discretization that "floats" over the fluid mesh. Instead of deforming the fluid mesh to match the structural boundary, the presence of the solid is accounted for by adding a localized body force to the momentum equations. While IBM is exceptionally robust for problems involving complex, moving geometries with large displacements, it lacks the near-wall resolution of ALE.

To summarize the fundamental differences between these methodologies, Table 5 provides a comparative analysis based on accuracy, cost, and topological flexibility. As the comparison suggests, ALE remains the premier choice for boundary-layer-sensitive problems like FSI in turbines, whereas interface-capturing or non-conforming methods are prioritized when the problem involves massive changes in topological connectivity.

Table 5: Comparative analysis of ALE versus interface-capturing (VOF/Level-Set) and non-conforming (IBM) methodologies.

Feature	**ALE**	**VOF / Level-Set**	**IBM**
Interface Accuracy	**Excellent**	Moderate	Moderate
Topology Change	**No**	**Yes**	Yes (with effort)
Boundary Layers	**Accurate**	Diffused	Difficult
Mesh Motion Cost	High	None	None
Best For:	FSI, Turbines	Breaking Waves	Heart Valves

11 Final Synthesis and Conclusions

The Arbitrary Lagrangian–Eulerian (ALE) description represents more than just a numerical technique; it is a unified continuum framework that bridges the classical divide between fluid and solid mechanics. Throughout this technical exposition, we have traced the development of this framework from its kinematic foundations to its complex application in fluid–structure interaction. As a retrospective of this conceptual flow, Figure 11 illustrates the logical progression from the necessity of moving domains to the numerical realization of the Geometric Conservation Law.

The integrity of this framework rests upon four primary pillars. First is the **Mapping** $\boldsymbol{\chi}$, which mathematically decouples material points from grid points. Second is the **Mesh Velocity** $\mathbf{w}$, providing the freedom to move the grid independently of the physical flow. Third is the **Convective Velocity** $(\mathbf{v}-\mathbf{w})$, which redefines transport in every conservation law (mass

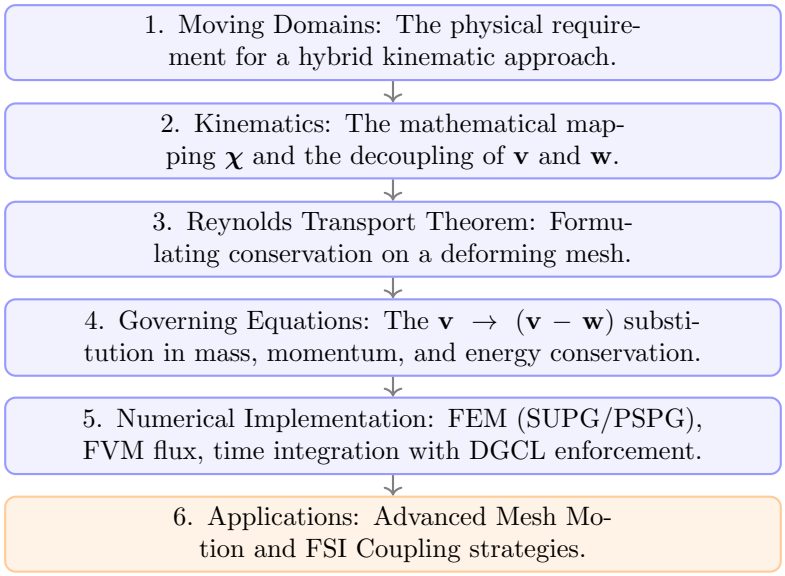

Figure 11: Conceptual flow and structural hierarchy of the ALE framework development.

(41), momentum (44), and energy (47)) within the moving frame. Finally, the **Geometric Conservation Law** (49) and its discrete counterpart (53) provide the consistency condition that prevents geometric evolution from introducing non-physical source terms. Together, these pillars enable the solver to maintain a body-conforming interface while regularizing the interior mesh, resolving thin boundary layers with a degree of precision that interface-capturing methods cannot easily match.

On the numerical side, the ALE weak formulation is directly compatible with stabilized finite element methods: the SUPG and PSPG stabilizations extend from the fixed-grid setting by replacing the material velocity with the relative velocity $\mathbf{c}$ in the stabilization parameter τ. In the finite volume framework, the ALE flux $\mathcal{F}_f = \phi_f(\mathbf{v}_f - \mathbf{w}_f) \cdot \mathbf{n}_f A_f$ encodes the same substitution at the discrete face level, and the DGCL provides the consistency condition that synchronizes the flux computation with the cell-volume update. Mesh motion requires an additional choice among spring analogy, Laplacian smoothing, or elastic analogy strategies, each reflecting a different balance between robustness, computational cost, and mesh quality as measured by the Jacobian, aspect ratio, and skewness metrics.

The central observation of ALE transport theory is that every conservation law must account for the "swept volume" of moving cell faces. The relevant transport velocity is always the relative velocity $\mathbf{c} = \mathbf{v} - \mathbf{w}$, not the material velocity alone. In this sense, the ALE approach transforms the simulation into a coupled problem: one must solve not only for the fluid state $(\mathbf{v}, p)$, but also for the mesh motion field itself.

Looking forward, the ALE framework continues to evolve along several active research directions. Machine learning is being applied to predict optimal mesh motion and prevent element tangling in complex geometries. High-order ALE methods based on Spectral Element or Discontinuous Galerkin discretizations are being developed to maintain GCL compliance at high accuracy levels. There is also continued interest in space–time formulations [Tezduyar et al., 1992], where time is treated as a fourth spatial dimension to construct a truly unified moving mesh, and in hybrid ALE-VOF methods that combine the interface-fitting precision of ALE with the topological flexibility of Volume-of-Fluid for problems involving surface breakup.

Acknowledgements

The research is financed by the Swedish Transport Administration in the project "GEneric Multidisciplinary optimization for sail INstallation on wInd-assisted ships" (GEMINI, Grant No. TRV 2023/32107). The computations and data handling were enabled by resources provided by the National Academic Infrastructure for Supercomputing in Sweden (NAISS), partially funded by the Swedish Research Council through grant agreement no. 2022-06725.

References

J. T. Batina. Unsteady Euler airfoil solutions using unstructured dynamic meshes. *AIAA J.*, 28(8):1381–1388, 1990. doi: 10.2514/3.25229.

A. N. Brooks and T. J. R. Hughes. Streamline upwind/Petrov–Galerkin formulations for convection dominated flows with particular emphasis on the incompressible Navier–Stokes equations. *Comput. Methods Appl. Mech. Eng.*, 32(1–3):199–259, 1982. doi: 10.1016/0045-7825(82)90071-8.

P. Causin, J.-F. Gerbeau, and F. Nobile. Added-mass effect in the design of partitioned algorithms for fluid–structure problems. *Comput. Methods Appl. Mech. Eng.*, 194(42–44):4506–4527, 2005. doi: 10.1016/j.cma.2004.12.005.

J. Donea and A. Huerta. *Finite Element Methods for Flow Problems*. John Wiley & Sons, Chichester, 2003. doi: 10.1002/0470013826.

J. Donea, S. Giuliani, and J. P. Halleux. An arbitrary Lagrangian–Eulerian finite element method for transient dynamic fluid–structure interactions. *Comput. Methods Appl. Mech. Eng.*, 33(1–3):689–723, 1982. doi: 10.1016/0045-7825(82)90128-1.

J. Donea, A. Huerta, J.-P. Ponthot, and A. Rodríguez-Ferrán. Arbitrary Lagrangian–Eulerian methods. In E. Stein, R. de Borst, and T. J. R. Hughes, editors, *Encyclopedia of Computational Mechanics*, volume 1, chapter 14. John Wiley & Sons, Chichester, 2004. doi: 10.1002/0470091355.ecm009.

C. Farhat, P. Geuzaine, and C. Grandmont. The discrete geometric conservation law and the nonlinear stability of ALE schemes for the solution of flow problems on moving grids. *J. Comput. Phys.*, 174(2):669–694, 2001. doi: 10.1006/jcph.2001.6932.

C. W. Hirt and B. D. Nichols. Volume of fluid (VOF) method for the dynamics of free boundaries. *J. Comput. Phys.*, 39(1):201–225, 1981. doi: 10.1016/0021-9991(81)90145-5.

C. W. Hirt, A. A. Amsden, and J. L. Cook. An arbitrary Lagrangian–Eulerian computing method for all flow speeds. *J. Comput. Phys.*, 14(3):227–253, 1974. doi: 10.1016/0021-9991(74)90051-5.

T. J. R. Hughes, W. K. Liu, and T. K. Zimmermann. Lagrangian–Eulerian finite element formulation for incompressible viscous flows. *Comput. Methods Appl. Mech. Eng.*, 29(3):329–349, 1981. doi: 10.1016/0045-7825(81)90049-9.

T. J. R. Hughes, L. P. Franca, and M. Balestra. A new finite element formulation for computational fluid dynamics: V. Circumventing the Babuška–Brezzi condition: a stable Petrov–Galerkin formulation of the Stokes problem accommodating equal-order interpolations. *Comput. Methods Appl. Mech. Eng.*, 59(1):85–99, 1986. doi: 10.1016/0045-7825(86)90025-3.

A. A. Johnson and T. E. Tezduyar. Mesh update strategies in parallel finite element computations of flow problems with moving boundaries and interfaces. *Comput. Methods Appl. Mech. Eng.*, 119(1–2):73–94, 1994. doi: 10.1016/0045-7825(94)00077-8.

M. Lesoinne and C. Farhat. Geometric conservation laws for flow problems with moving boundaries and deformable meshes, and their impact on aeroelastic computations. *Comput. Methods Appl. Mech. Eng.*, 134(1–2):71–90, 1996. doi: 10.1016/0045-7825(96)01028-6.

S. Osher and J. A. Sethian. Fronts propagating with curvature-dependent speed: algorithms based on Hamilton–Jacobi formulations. *J. Comput. Phys.*, 79(1):12–49, 1988. doi: 10.1016/0021-9991(88)90002-2.

C. S. Peskin. The immersed boundary method. *Acta Numer.*, 11:479–517, 2002. doi: 10.1017/S0962492902000077.

T. E. Tezduyar, M. Behr, and J. Liou. A new strategy for finite element computations involving moving boundaries and interfaces—the deforming-spatial-domain/Space–Time procedure: I. The concept and the preliminary numerical tests. *Comput. Methods Appl. Mech. Eng.*, 94(3): 339–351, 1992. doi: 10.1016/0045-7825(92)90059-S.